MASTERARBEIT | MASTER'S THESIS

Titel | Title

Photosynthetic capacity and carotenoid content of the terrestrial algae Trentepohlia aurea

verfasst von | submitted by

Andrea Mussone

angestrebter akademischer Grad | in partial fulfilment of the requirements for the degree of

Master of Science (MSc)

Wien | Vienna, 2024

Studienkennzahl lt. Studienblatt | Degree programme code as it appears on the student record sheet:	UA 066 833
Studienrichtung lt. Studienblatt | Degree programme as it appears on the student record sheet:	Masterstudium Ecology and Ecosystems
Betreut von | Supervisor:	ao. Univ.-Prof. Mag. Dr. Michael Schagerl

MASTERARBEIT/MASTER'S THESIS

Titel der Masterarbeit / Title of the Master's Thesis

Photosynthetic capacity and carotenoid content of the terrestrial algae *Trentepohlia aurea*

Verfasst von / submitted by

Andrea Mussone

Angestrebter akademischer Grad / in partial fulfilment of the requirements for the degree of

Master of Science (MSc)

Wien, 2024 / Vienna, 2024

Studienkennzahl It. Studienblatt / Degree Programme code as it appears on The student record sheet:	UA066 833
Studienrichtung It. Studienblatt / Degree programme as it appears on The student record sheet :	UG2002

Betreut Von / Supervisor : ao. Univ. Prof. Mag. Dr. Michael Schagerl

Abstract

Trentepohlia aurea due to its extremely high carotenoid content has been proved to be an interesting taxon to study for commercial exploitation. Characteristics such as the aero terrestrial habitat, tolerance to desiccation and synthesis of valuable compounds such as β-carotene, vitamine C and vitamine E make it a promising taxon for research. We studied maximum quantum yield of photosystem II and cellular carotenoid vesicle volumes of *T. aurea* under different treatments (BG11, BG11 at 1/10 of concentration and BG11 nitrogen depleted) Significant differences between cultures treated in N-limitations conditions and other treatments were found, where *T.aurea* displayed a considerably higher maximum quantum yield of PSII and a increase in total carotenoids number. Furthermore, different substrates were tested (agar and marmolade), as a result, marmolade proved to be the best substrate to grow the algae. Observations of the chloroplast and carotenoids locations within the cells by means of Confocal laser scanning microscopy allowed us to calculate the carotenoids cellular vesicle volumes. Furthermore, hereby we provide a framework for the measurements of carotenoids vesicles volume by acquiring stack images with confocal microscope and their elaboration utilizing ImageJ.

Introduction

Morphology, life history and carotenoids function in the genus *Trentepohlia*

Trentepohlia is a common genus within the Ulvophyceae (Chlorophyta) found on woods, barks, leaves and rocks (Fritsch 1935, Ho et al. 1983, Chapman 1984). Seemingly as observed in this study, species of the genera *Trentepohlia* can be found in the near vicinities of freshwater courses. Characterizing and studying organisms belonging to Sweetwater flora has become increasingly important. In recent years freshwater flora is facing a number of issues. Among others, climate change is and will alter primary production in freshwater bodies, increasing pulsed nutrients supply, solute concentrations and altering stratification regimes (Downing 2014). Mismanagement of wastewaters, altering the physio – chemical and biological characteristics of freshwater bodies, damaging permanently aquatic and associated biota (Mushtaq et al. 2020). The genus comprises about 40 species (Hoek et al. 1995) that are typical members of the subaerial vegetation present in tropical and subtropical areas (Fritsch 1907). A few species are also common in temperate regions (Printz 1964). *Trentepohlia* is thought to have good tolerance and high adaptivity to physiological stresses such as desiccation and high temperature. In the last two centuries, many studies have been carried out on various biological aspects. Research has been undertaken covering morphology, distribution and reproduction (Printz 1939), physiology (Howland 1929, Tan et al. 1993, Abe et al. 1999), photosynthesis (Ho et al. 1983, Ong et al. 1992) and ultrastructure (Graham and McBride 1975, 1978, Chapman and Good 1978, Roberts 1984, Chapman et al. 2001).

Trentepohlia is generally characterized by its filament morphology and different cellular structures, the absence of pyrenoids in the chloroplasts, a flagellar apparatus with unique structure, a transverse cells wall with plasmodesmata and differentiated reproductive cells (Rindi et al. 2009, López-Bautista et al. 2002). However, specific growth conditions to maintain healthy cells make *Trentepohlia* difficult to work with and consequentially several aspects of their biology have not been elucidated yet. Moreover, morphology changes considerably within species, which makes identification a challenge; some species are regarded as highly polymorphic (Harriot 1889, Printz 1939, 1964, Rindi and Guiry 2002). Taxonomic criteria are based on cell shape and size (length and width) on vegetative cells, branching pattern, position and morphology of reproductive structures and presence of hair – like cells (De Wildeman 1888, Hariot 1889, Printz 1921, 1939, 1964). These characteristics are, however, highly variable and depending on prevailing environmental conditions (Thompson and Wujek 1997). Furthermore, life history is another aspect not yet completely clear: it is currently presumed that life cycles consists of an isomorphic alternance of diploid sporophytes producing quadriflagellate meiospores and haploid gametophytes producing biflagellate gametes, which fuse isogamously (Wille 1878, Oltmanns 1923, Printz 1964, Thompson and Wujek 1997) Evidence of this, however is inconclusive (Hoek et al. 1995). All the Trentepohliaes have filamentous growth forms usually containing large number of carotenoids giving the algae a reddish-yellow colour (Thomson and Wujek 1997, Lo´pez-Bautista et al. 2002). Production and characterization of carotenoids in the genus *Trentepohlia* have been documented in different species. For example, Voytsekhovich and Kashevarov (2010) analysed the content of

chlorophylls a and b, β-carotene and xanthophylls in *Trentepohlia umbrina*, showing low quantities of chlorophylls with respect to the carotenoid content. Abe et al. (1998, 1999) demonstrated the production of vitamins C and E and carotene in *Trentepohlia aurea*. Kharkongor and Ramanujam (2015) proved the presence of cryptoxanthin, lutein and β – carotene in *T. umbrina*. Carotenoids have been assigned a number of function in higher plants and algae. Carotenoids quench the excited state of chlorophyll, acting both as energy donors and energy acceptors (Owens et. 1992). By acting as a filter, especially at high altitudes carotenoids are accumulated in cover tissues of plants, inactivating near ultraviolet and blue incident light which may inhibit the functional photosynthetic apparatus (Ladygin 2014). Protecting against the photo destruction of membrane lipids, carotenoids such as xanthophyll, when in presence of oxygen prevents lipids degradation, providing stability to the thylakoid membrane at high light intensity (Klyachko-Gurvich et al. 2000). Antioxidant activity through the protection of the photosynthetic apparatus against photooxidative damage (Havaux et al. 2007), Zeaxanthin for example due to its oxidative capacity has been observed to facilitate membrane stabilization at high temperature by quenching triplets chlorophyll (Havaux and Niyogi 1999). During long periods of water stress, low temperatures and nutrient deficiencies, accumulations of antheraxanthin and zeaxanthin were found in nocturnal hours to may prevent photochemical damage in the morning (Barker et al. 2002). In *Trentepohlia gobii* for instance, large amounts of β - Ɛ carotene and β - β carotene and all their derivates should have a protective role (Czeczuga and Maximov 1996). Therefore, due to the interesting properties and function of carotenoids in higher plants and algae, it was of interest in our study to investigate new techniques to quantify their amount and how to increase their production.

Specific studies on *Trentepohlia aurea*

Literature regarding *Trentepohlia aurea* is scarce. In the last years, a few studies focused on specific properties and possible industrial applications. Abe et al. (2002) suggested how *Trentepohlia aurea* was able to remove nitrate, nitrite or ammonium and phosphate from synthetic wastewater (a medium with considerably high concentrations of N and P ions). However, the outcome of the study needs to be scrutinized as the authors probably misidentified the taxon (*T. aurea* occupies a narrow ecological niche in terrestrial environments, therefore it is unlikely it could grow and thrive in a water medium). Other studies have examined the production of carotenoids in CO_2-enriched cultures. Abe et al. (1999) focused on the synthesis of valuable compounds such as vitamins and E and β – carotene in culture media enriched with 5% CO_2, suggesting the presence of a carbon transporter, probably HCO_3^- transporter, located in the cell membrane. The study suggests how the algae could be used as bio-functional material for reducing industrial CO_2 and perhaps NO_x and SO_x or for making a greenbelt over concrete surface on highways. Gupta & Agrawal (2004) tested *Trentepohlia aurea* vegetative cells ability to survive prolonged exposure in water and air, respectively. Vegetative cells could not survive for more than 5 months under submerged condition, showing disintegration and death without sporangium formation. Furthermore, they tested the tolerance against salt, pesticides and heavy metals. *Trentepohlia aurea* vegetative cells were able to tolerate to some extent $NaCl \leq 0.8$ mol L^{-1}, pesticides (DDT, 2,4-D or captan, 2000 ppm) and heavy metals (zinc or nickel, 200 ppm; cobalt, ≤100 ppm.). Mukherjee et al. (2010) provided new information on the biosynthesis of carotenoids in *T. aurea* and *T. cucullate* without culturing the algae in any

medium. The carotenoids found were the following: Neoxhantin, Lutein, β-cryptoxanthin, β,γ-carotene, β,ε-carotene, β.β-carotene. Holzinger et al. (2023) assessed *Trentepohlia aurea* photosynthetic activity and its resistance to desiccation comparing it with two other species *Trentepohlia umbrina and Trentepohlia jolithus.* The authors found that *T. aurea* displayed the highest photosynthetic activity, the highest P_{max} and the lowest alpha values indicating effective light use already at low irradiances without signs of photoinhibition at high irradiances. However, the taxon had lowest tolerance against desiccation. The study concluded that the species investigated differed quantitatively and qualitatively in the level of polyol composition, which is an important compound with an active role in protecting against various stress conditions.

Graham and McBride (1975) investigated the multilayered structures (MLS of flagellates of *Trentepohlia aurea* underlying some of its peculiar characteristics. First, the connection of the basal body and the MLS seem to be an electron-dense material which caps the base of each flagellum. Second, the basal body of *T. aurea* are never seen positioned over a MLS, sections of one or both MLS are found at the side of cross sections of the basal bodies. Third, *Trentepohlia aurea* has likely one of the simplest MLS described in comparison to the number of microtubules in the first layer; the motile cells of *Trentepohlia* are one of the smallest MLS containing cells. Fourth, *Trentepohlia aurea* cytoskeleton is symmetrical; in fact it suggests the presence of a primitive cytoskeleton linked with algae possessing symmetrical roots but not MLS. Manton (1966) suggested that symmetry in the flagella apparatus might be of importance for phylogenetic studies.

Quantum yield of photosystem II

The photosynthetic apparatus of eukaryotic algae, vascular plants and cyanobacteria is found in the specialized thylakoid membrane system, mediated by the integral membrane protein complex photosystem II (PSII), cytochrome b6/f, photosystem I (PSI), and ATP synthase. The protein complex has the function of harvesting light and transforming solar energy into chemical energy (Eberhard et al. 2008). Giving the importance of these processes, measuring and quantifying their efficiency has become increasingly important over the last years. In the past decades, the influence of stress on plant photosynthetic activity has gained widespread interest (Schulze and Caldwell 1994). Using pulses of strong light called saturation pulse, the factors characterizing fluorescence yield can be analysed (Bradbury and Baker 1981, Quick and Horton 1984, Dietz et al. 1985, Schreiber et al. 1986). Chlorophyll fluorescence has become a valid alternative to measure the photophysiology of plants. The development of fast repetition rate fluorometer (FRRF) and pulse amplitude modulation (PAM) in the 1980s permitted the measurement of photosynthesis in marine plants (Schreiber et al. 1995). The PAM method allows to monitor chlorophyll fluorescence without inducing photosynthesis, based on a weak modulated measuring light pulse.

There are several photosynthetic parameters applicable to determine the photosynthetic capacity of plants. Pulse amplitude modulation fluorometers are able to measure effective quantum yield Y(II) during light exposure calculated with the following formula: $(F_m' - F)/F_m'$ and maximum quantum yield of PSII (Φmax PSII) in the dark calculated with the following formula: $F_v/F_m = (F_m - F_o)/ F_m$ (Genty et al. 1989). F_m' is equivalent to maximal fluorescence yield during illumination, F_m dark-acclimated maximal fluorescence yield, F_v variable

fluorescence yield, F_o dark acclimated minimal fluorescence yield and F, the normal fluorescence. Quantum yield is defined as the number of defined events which occur per photon absorbed by the system or as the amount of mol of reactant consumed or product formed per amount of photon (einstein) absorbed (Verhoeven 1996). Empirical indices were derived which have proven to be suitable for the quantification of PS II efficiency (Butler 1978; Weis and Berry 1987; Genty et al. 1989). Moreover, Φmax PSII and Y(II) differs in the following: the Y(II) can vary greatly depending on the environmental factors such as substrate moisture and light conditions (O'Neill et al. 2006, Murchie and Lawson 2013, Hazrati et al. 2016, Lang et al. 2018). On the other hand, Y(II) is a great parameter to use in field experiments as it does not require the sample to be in dark conditions (Brestic and Zivcak 2013). Furthermore, by measuring Y(II) is possible to calculate the electron transportation rate (ETR) which is derived by the Y(II). In the photosynthetic process, ETR is involved in different pathways. ETR generates energy (ATP) and reducing power (NADPH) both required for the photosynthetic carbon reduction and for the photorespiratory carbon oxidation (Cheng et al. 2001, Nelson and Yocum 2006). Indeed ETR directly or indirectly (through electron exchange and the provision of ATP) is tied to additional pathways such as the reduction of O_2 in the Mehler reaction (Asada 1999, 2000, Badger et al. 2000, Ort and baker 2002), nitrate reduction (Turpin et al. 1988, Cheng et al. 2001, Eichelman 2011) and terminal oxidases (Streb et al. 2005, Biley et al. 2008, Miyake 2010, Hemschemeier and Happe 2011). Because of these reasons, biophysical processes driving ETR are essential in maintaining an optimal photosynthetic rate and providing a correct flow of ATP and NAPH to the pathways needed to fix inorganic carbon into organic skeletons for either maintenance or growth. On the other hand Φmax PSII can be used to evaluate the efficiency of the PSII and to calculate eventual stressor leading to a reduction of quantum yield activity in the photosystem II (Demmig and Bjrkman 1987, Schreiber and Bilger 1993). It is because of the useful implementation of Y(II), ETR and Φmax PSII, that these parameters were considered in our study to asses respectively, the health conditions of the algae depending on the environmental parameters, and to asses the overall health conditions of the cultures under the treatments tested.

Confocal laser scanning microscopy (CLSM)

Techniques of laser scanning and spinning disk confocal fluorescence microscopy has become an essential tool in different disciplines such as biology, biomedical science and material science. This is due to attributes that are not yet available using other contrast mode with traditional optical microscopy (Centonze and Pawley 1995, Masters 1996). Modern confocal microscopes can be considered as a complete electronic system where the optical microscope plays a central role in the configuration consisting of several components such as one or more electronic detectors, a computer (for image display, processing, output and storage), and several laser systems combined with wavelength selection devices and a beam scanning assembly (Claxton et al. 2006). Confocal microscopes are now used for routine investigations on molecules, cells and living tissues that were not possible just a few years ago (Goldman and Spector 2005). The CLSM offers different advantages over the conventional widefield optical microscopy including the ability to control depth of field, elimination or reduction of background information away from the focal plane and the ability to collect serial optical sections from thick specimens (Claxton et al. 2006). Giving the efficacy of the confocal

microscope and its widespread utilization in analysing cell structures and molecules. In this study, we analysed and characterised the total carotenoids volume within *Trentepohlia aurea* via CLSM, supporting the thesis that the carotenoids volume change according to the treatments given.

Material and methods

Sampling site

Trentepohlia aurea measurements were performed in Lunz am See, Austria in two different locations. One of the two locations was situated close to the parking lot of the research station WasserCluster Lunz. The current site is characterized by being considerably exposed to the sun, especially over afternoon hours. GPS coordinates and cardinal direction were evaluated with a compass, latitude resulted to be 47°.8515806 N and longitude 15° .0419903 W. with the algae direction being 342.0° North at a latitude of 622m. considering the site was characterized by being situated on a concrete wall in proximity of asphalt, the site is named “artificial site” (Figure 1). The second location was located close to a river, in the woods nearby the research station In Lunz am See, this location was characterized by having great vegetation cover due to trees canopies in near proximity, with the algae growing on a rocky substrate (Figure 2). The coordinates are the followings: latitude 47°.8528615 and longitude 15.0656495, with the algae direction being 343.6° North at a latitude of 622m. Due to the location being great in vegetation cover and far from human settlements, the site is called “natural site”. The measurements in both sites were performed with different weather conditions, during sunny – dry and rainy – humid days.

Environmental Parameters

Measurements of air temperature, dew point, relative humidity and irradiance were collected in both sites. Relative humidity and dew point were both measured with the device sensor located on the surface of the in the artificial site and on the rocky surface in the natural site. The measurements were performed every ten minutes over three consecutive days, over night and day light.

Physiological Parameters

Physiological parameters were evaluated by measuring Y(II) and ETR utilizing a DIVING – PAM II device from Walz. In order to calculate the Y(II), first Fm' and F are measured and then, Y(II) was calculated in the following way: $(Fm' - F)/Fm'$. Once the Y(II) was measured then, ETR was derived with the following calculation: ETR = Y(II) * 0.85 * R * PAR, where R = 0.05 is a constant and PAR is the active radiation measured in $\mu mol \cdot m^{-2} \cdot s^{-1}$. The PAM sensor was positioned at a 45º angle beneath the algae, in order to allow the incident light to

reach the colonies, therefore, to calculate Y(II). In both the sites the measurements were performed every ten minutes for a total of three days each.

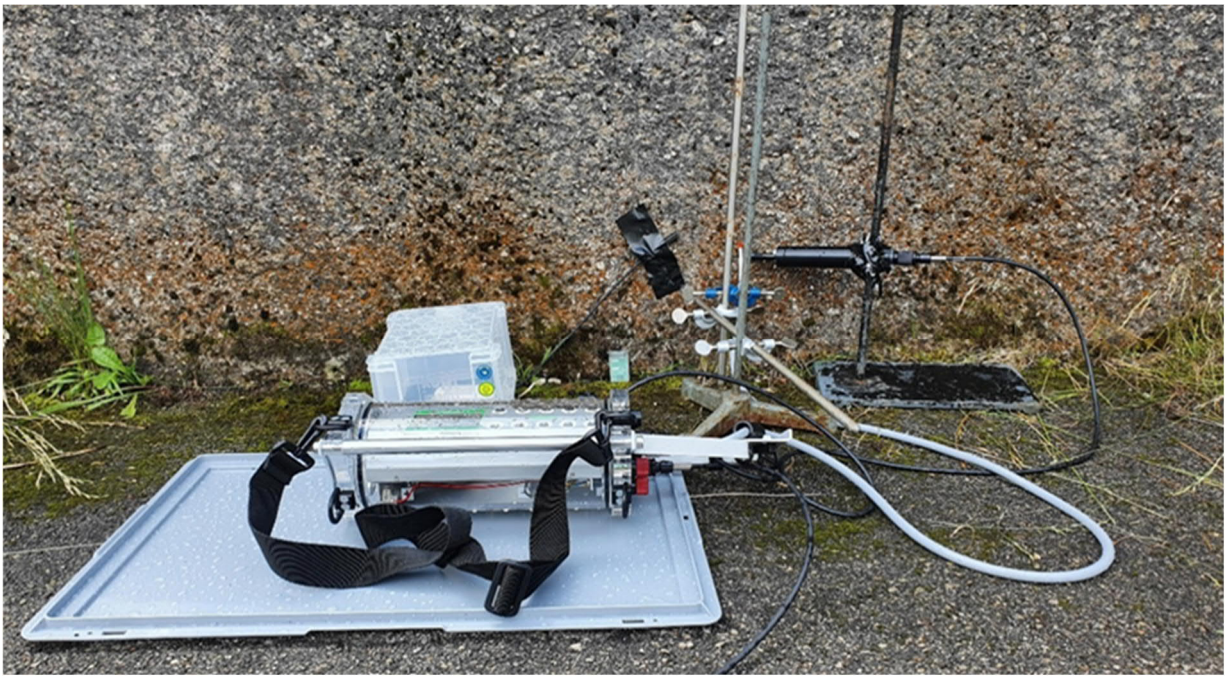

Figure 1 1: Artificial site. *Trentepohlia aurea* was barely present on the wall with few spots suitable for performing the measurements

Figure 2: Natural site with *Trentepohlia aurea* growing on several stones (carbonate rocks). The algae are in healthy condition, performing well all over the rocks.

Growth condition assessments in the laboratory

Specimens of *Trentepohlia aurea* were scratched with a spoon from the surface of rocks located in the natural site. The samples were then transported in a cooling bag to the phycology laboratory at the university of Vienna, and finally stored in a fridge at 3ºC. 5 replicates per treatment were prepared in small petri dishes, as substrate two different substrates were tested: (1) open and closed petri dishes were prepared with agar at a concentration of 1,5% containing the growth medium. Closed petri dishes were wrapped all around with parafilm. 2) open petri dishes containing marmolade. The medium used to treat the cultures were the following: modified BG11 medium, (table 1) (Rippka and Herdman 1992), $NaNO_3$ depleted BG11 labelled as BG11_0 , BG11_1 with just 1/10 concentration of full BG11 and rain water (R.w). The cultures were stored in a cultivation chamber set up at 18ºC with a cycle of 16 hours of light and 8 hours of darkness and a light intensity between 20 $\mu mol \cdot m^{-2} \cdot s^{-1}$ and 40 $\mu mol \cdot m^{-2} \cdot s^{-1}$. Treatments were provided via spraying repeatedly on the cultures every day. The Experiment duration was of 31 days, the Φmax PSII was measured every second day. To analyse the Φmax PSII , the samples were kept in dark condition for thirty minutes before each measurement. Measurements were performed twice, before and after spraying in order to assess whether there was an increment in the Φmax PSII after providing the treatments. At the end of the experiment, a light microscopy inspection was conducted on the cultures in order to assess by naked eye the amount of carotenoids, new cell formations, the presence of reproductive structures and eventual contaminations in the samples, seeking for difference between treatments. Furthermore, the samples were photographed every second day in order to display the presence of visible morphological change in the samples depending on the treatments.

Table 1: BG11 medium composition

Reagents	Stock solution [g/100ml]	Nutrient solution [ml]
$NaNO_3$	15	5
K_2HPO_4. $3H_2O$	0.4	5
$MgSO_4$. $7H_2O$	0.75	5
$CaCl_2$. $2H_2O$	0.36	5
Citric acid	0.06	5
Ferric ammonium citrate	0.06	5
EDTA (dinarium – salt)	0.01	5
Na_2CO_3	0.2	5
Micronutrient solution		0.5
De-ionized or distilled water		460

Assessment of the cellular carotenoid volume

CLSM Observation and image capturing

Measurements of the carotenoid volume were performed utilizing a Leica SP8 confocal microscope using the software LAS X office. Microscopical observations were conducted on days 1, 10, 21. During each observation, 3 cells per each treatment were analysed. Utilizing the Leica software, stack pictures were taken and then analysed with the open-source software ImgaeJ (Rasband 1997-2018). Additionally, to the carotenoids globules volume and chloroplasts were analysed in order to inspect the cellular organelles and to provide further details on the cell structure. To perform the analysis, the argon laser was utilized. In order to obtained detailed and clean pictures, a Lambda scan with each laser line was performed before the measurements. The laser line tested were the following: 405, 458, 476, 488, 496 and 514. The laser line 405 demonstrated to have too short wavelengths for the carotenoids, therefore not applicable for their analysis, demonstrating however good emission intensity for the chloroplasts being between 600 nm and 650 nm. The laser line 458 excited the chloroplasts at a wavelength between 659 nm – 700 nm , showing no emission regarding the carotenoids. The laser line 476 showed good excitation for both the carotenoids and the chloroplasts, with an emission range between 495 nm – 575 nm, and 650 nm – 700 nm, respectively. The laser line 488 showed good excitation for both carotenoids (500 nm – 600 nm) and chloroplasts (650 nm-700 nm). The laser line 496 showed a good emission regarding the chloroplasts (655 nm-710 nm), showing to be the best laser to excite the chloroplasts but having poor performance on the carotenoids. Laser line 514 showed good emission on carotenoids (530 nm-570 nm), but no excitation for the chloroplasts was detected.

ImageJ anaylsis

Thresholding and images elaboration

The stack images obtained with the confocal microscope had been elaborated with the open-source software ImageJ (Rasband 1997-2018). In order to elaborate the stack images and making them suitable for the analysis, each image has been modified with the same criteria, in order to obtain reproducible results for comparisons. Using the command “rotate” (image – transform – rotate), the images were rotated to cut out areas of the image not being considered. Secondly by selecting a portion of the image and then with the command “auto-crop” (image – adjust – auto crop), specific areas of the image were selected for analyses. Thirdly, to every image the filter “Gaussian Blur 3D” was applied (Process – filters – Gaussian Blur 3D). The filter aforementioned is useful when analysing noisy pictures, the filter blurs the noise, making the background more distinguishable from the region of interest. Fourthly with the command “threshold” (image – adjust – threshold), for each image a different threshold was applied with the following options checked: “Stack histogram”, “Dark background” and “Don’t reset range”. Thresholding is a procedure used in image analysis in order to select pixels based on the intensities of the pixels values. Once an intensity value is set, every pixel below the defined value will be ignored, instead the pixels equal or above the defined threshold will be calculated. This practice is particularly useful to select the region of interest to analyse. The option “stack

histogram checked" enables the software to calculate the threshold based on the histogram of the entire stack and not only from the 2D image currently displayed (Bankhead Pete 2022-2024). When adjusting the threshold, ImageJ offers different automatic thresholds, each threshold is distinguished by a different algorithm (IsoData, Maximum of entropy, Otsu etc..). Among all the auto threshold methods available, "Otsu" was chosen for the measurement of every image. "Otsu" divides pixels in two classes, bright and dark, then it calculates the average pixel values, assigning threshold values at the midpoint between bright and dark pixels. This is an effective way to threshold foreground object from the background (Otsu 1975). However, in order to test the effectiveness of other threshold options with the command auto-threshold (image – adjust – auto threshold), the effectiveness of each auto threshold method was tested (Fig 3). Auto-threshold helps in deciding what auto threshold method is best to utilize to threshold the image, as some auto threshold methods do not recognise certain regions of the image. After defining a threshold with the command "slice remover" (image – stacks – tools – slice remover), slices containing elements outside the cellular space and other cells were removed. The following operation has been carried on with the threshold activated, in this way the area recognised by the threshold are coloured and it is easier to recognise portions that would otherwise being included in the measurements.

Figure 3: Image obtained with auto threshold command (image – adjust – autotreshold). The following image displays the same slice elaborated with different auto threshold methods.

3D detection methods performed

After elaborating the images, ImageJ offers three different ways to measure stack images and obtaining 3D measurements. To obtain the measurements data, each image has been analysed with three different methods, in order to find the most accurate and representative method for each image. The first method tested is carried on by creating a macro (plugins – new – macro). By inserting the code in Fig 4, the macro will loop through each image and will take

measurements of every slice individually fitting for each slice a different threshold value. Finally, the macro will loop through and sum all the measurements and multiplying this sum by the depth of each slide, eventually displaying the final results. The second methods utilised to measure 3D objects in ImageJ is within the option 3D objects counter (analyse – 3D objects counter). In order to decide the measurements to perform is necessary, through the command 3D OC options (analyse – 3D OC options) to select what parameters to measure. The options Volume, Surface, Integrated density, Centroid and Mean Gray value were checked. The command 3D object counter uses a single intensity threshold to divide a cell into two components cell (foreground) and non cell called background (Saphiro and Stockman 2001).

```
// ImageJ Macro Code
// Measure Volume of Thresholded Pixels in an Image Stack
//
//

macro "Measure Stack" {
    run("Clear Results");   // First, clear the results table

    // loop through each slice in the stack. Start at n=1 (the first slice),
    // keep going while n <= nSlices (nSlices is the total number of slices in the stack)
    // and increment n by one after each loop (n++)
    for (n=1; n<=nSlices; n++) {
       setSlice(n);  // set the stack's current slice to n
       run("Measure");   // Run the "Measure" function in ImageJ
    }

        // Create a variable that we will use to store the area measured in each slice
    totalArea = 0;
    // Loop through each result from 0 (the first result on the table) to nResult (the total number of results on the table)
    for (n=0; n < nResults; n++)
    {
       totalArea += getResult("Area",n);   // Add the area of the current result to the total
    }
    // Get the calibration information from ImageJ and store into width, height, depth, and unit variables.
    // We will only be using depth and unit
    getVoxelSize(width, height, depth, unit);
    // Calculate the volume by multiplying the sum of area of each slice by the depth
    volume = totalArea*depth;
    // Print the result of the volume calculation to the log
    print(volume + " " + unit + "^3");
}
```

Figure 4: code inserted under the section macro (plugins – new – macro) the following code allows ImageJ to calculate the surface of each slice of the stack image with a different threshold fitted for each slice to then measure the total volume of the stack analysed. The code showed was found on the website of the company VISIKOL (link in the reference as " Visikol")

The third and last method performed to measure the overall cellular carotenoids volume is the command "3D Manager" (plugins – 3D suite – 3D manager). In this command is possible to define a minimum and a maximum value to the threshold by selecting the command "segmentation" (Fig 5). By default, the low threshold value will be set at 128 and the maximum at 255. However, the low threshold value was set according to the automatic threshold value provided by the option "3D object counter" therefore the threshold was adjusted accordingly for each stack. Unlike the previous two detection methods performed, this command offers to inspect more accurately the object analysed. Once the segmented objects are added by activating the command "Live ROI" and "fill stack", the segmented image was inspected to check what portion of the image were analysed.

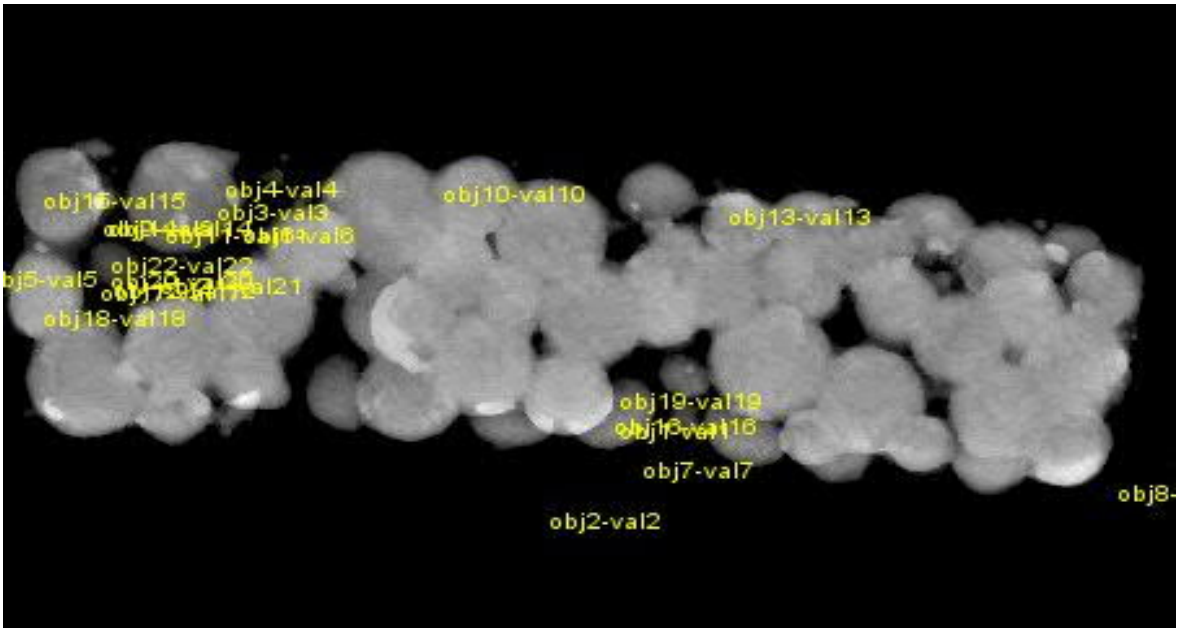

Figure 5: 3D reconstruction of the objects detected and analysed by the command 3D manager (voxels are labelled and numbered)

With the command 3D manager, is possible to see what object are analysed and selectively by the command “delete” all the objects that were not carotenoids were deleted in order to measure only the objects of interest. Furthermore, with the command “3D viewer” (figure 5), the figure was inspected to check whether or not the objects segmentation worked properly.

Carotenoids vesicle size measurements

Beside total carotenoids volume, the vesicle carotenoids size was estimated. Since carotenoids vesicle have a spherical shape, the diameter of the vesicle was evaluated and their circumference calculated ($C=2\pi r$) using the software LAS AF lite (Figure 6). In order to conduct the analysis a total of 10 vesicle per each cell analysed were measured. In total 3 cells per day each treatment was analysed resulting in a total of 30 replicate per treatment at each time point.

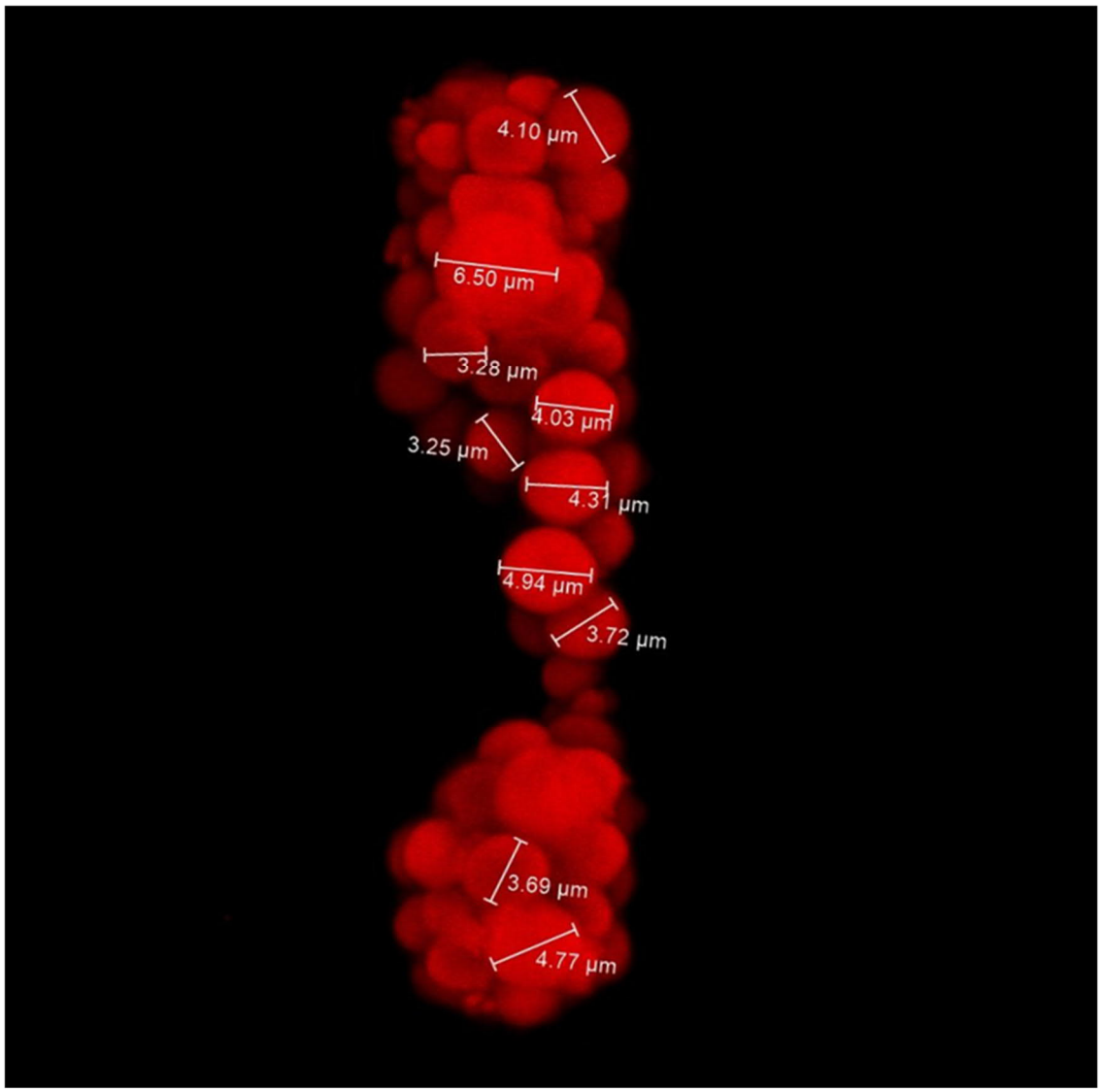

Figure 6: Evaluation of vesicle size using the software LAS AF lite. The measurement bars in the figure are showing the diameter of the vesicles

Statistical calculations

R statistical software (R core team. 2022) was used to perform all the statistical analysis. A two- way repeated measure ANOVA was performed in Fig 8, 11 and Fig 23 in order to asses statistical differences. In fig 8 it was tested if the location (natural or artificial) had effect on the Y(II) at each day (time point). In Fig 11 the test was utilized in order to assess if the ETR would change according to the Location, time, each time point was tested. On Fig 23 the test was performed in order to asses whether the carotenoids vesicle size would change according to the treatment at each time point. Furthermore, utilizing the package lme4 in R, in Fig 10, 11, 12 and 18 a linear mixed effect model (LMM) was fit in order to asses statistical differences. In Fig 10, the effect of relative humidity, dew point, irradiance and temperature were tested on the Y(II) in the natural and artificial sites looking for interactions effect between the variable on the Y(II). The LMM model in fig 11 was built testing the effect of the treatments on the Φmax PSII over the measurement days, moreover the LMM model displayed in Fig 13 was fit in order to look for statistical significance on the Φmax PSII between measurements performed before and after spraying the treatments over each time point. Finally in order to asses statistical differences between treatments on the total carotenoids volume (Fig 20) a LMM model was fit looking for statistical significance between the effect of the treatment on the total carotenoids volume at each time point.

Results

Field measurements

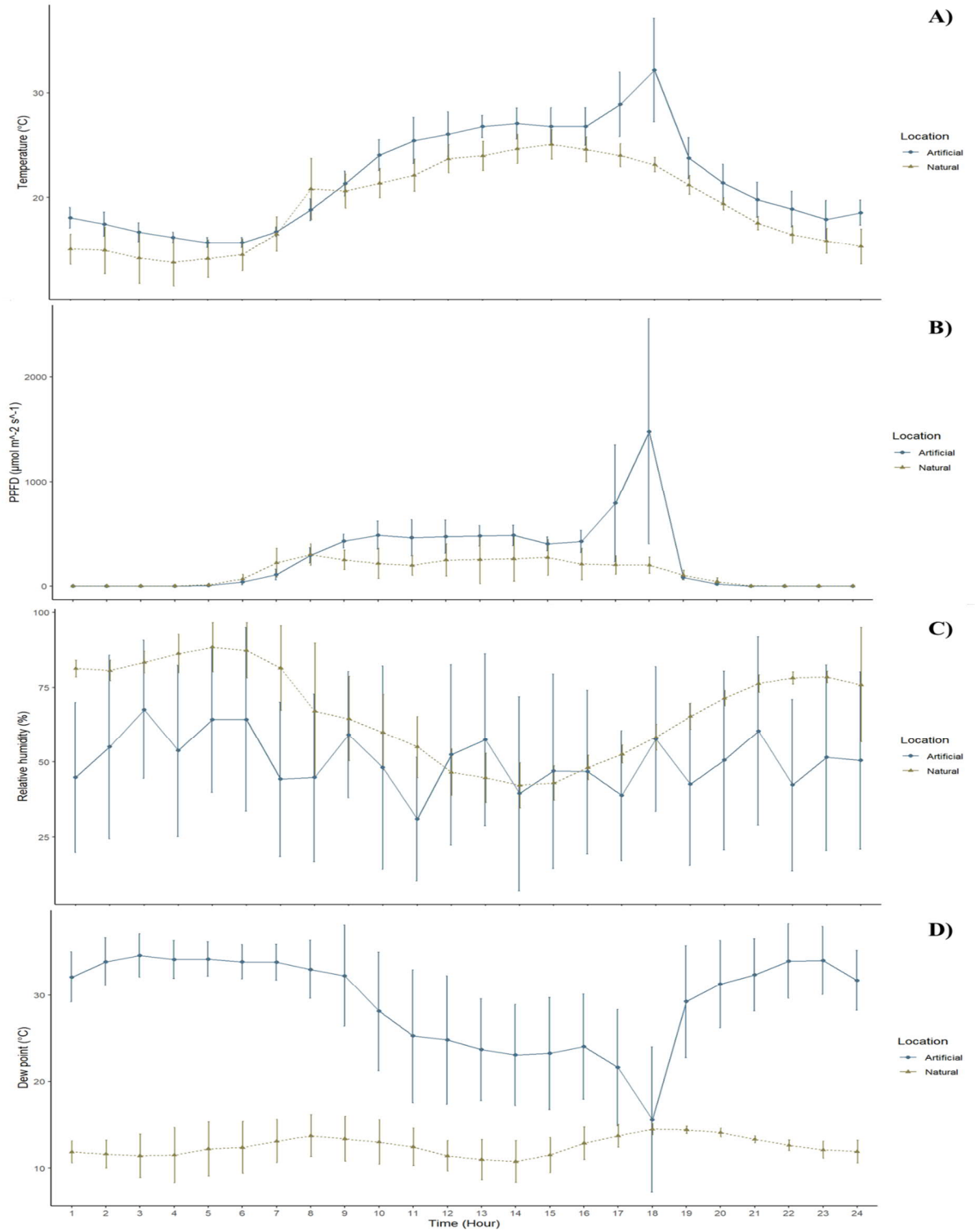

Figure 7: Environmental parameters change over hours across the artificial and natural sites. The following measurement are based on a three-day observation period in each site. Measurement in the artificial site were conducted from the 15/07/2022 to

the 18/07/2022 and in the natural site from the 22/07/2022 to the 25/07/2022. The data shown are based on the mean value of each environmental parameter considered, moreover, per each hour the standard deviation is calculated (notice error bars per each hour point).Calculation are based on 6 replicates per each hour, in total 730 replicates were anaylsed.

In figure 7 are displayed the environmental parameters measured in Lunz am see in two different sites labelled in dark blue and light blue. The environmental parameters measured are A) air temperature (°C), B) PPFD (µmol photons m^{-2} s^{-1}), C) relative humidity (%) and D) dew point (°C). When looking at the temperature data (figure 7 A) the two sites seem to have similar temperatures, the only difference being a pick in temperature at 18:00 in the artificial site reaching over 30°C. Light intensity was measured as well in both sites (Figure 7B), light intensity to differ between sites all over the diurnal hours, with artificial site being more exposed to sunlight, particularly is noticeable at around 18:00 when the light exposure reaches a pick in intensity around 1500 µmol m^{-2} s^{-1}. However, as displayed in the figure, the long error bar indicates a high data variability. On the other hand, light exposure in the natural site is tendentially higher just earlier in the morning at around 7:00 being however lower over the whole day. When looking at both Fig 7A and 7B it appears that the pick in temperature and light coincides at the same time (around 18:00). Relative humidity (Fig 7C) differs greatly between the two sites. In the natural site relative humidity displays overall higher values over the artificial site and is tendentially more linear, meanwhile in the artificial site, relative humidity is characterized by having more ups and downs all over the day, changing every hours. In either site, however, the highest relative humidity percentage is measured earlier in the morning between 3:00 and 5:00 being around 85%. Among all the parameters measured, dew point is the one being the most diverse across the two sites. In the natural site dew point is much lower and homogenous all over the day, moreover it is stable at around 12 °C. However in the natura site, the dew point fluctuates more over the day, being at its highest in the morning until 8:00 and over night (from 19:00 on) to then decrease from 9:00 to 18:00

Photophiyiological measurements in situ

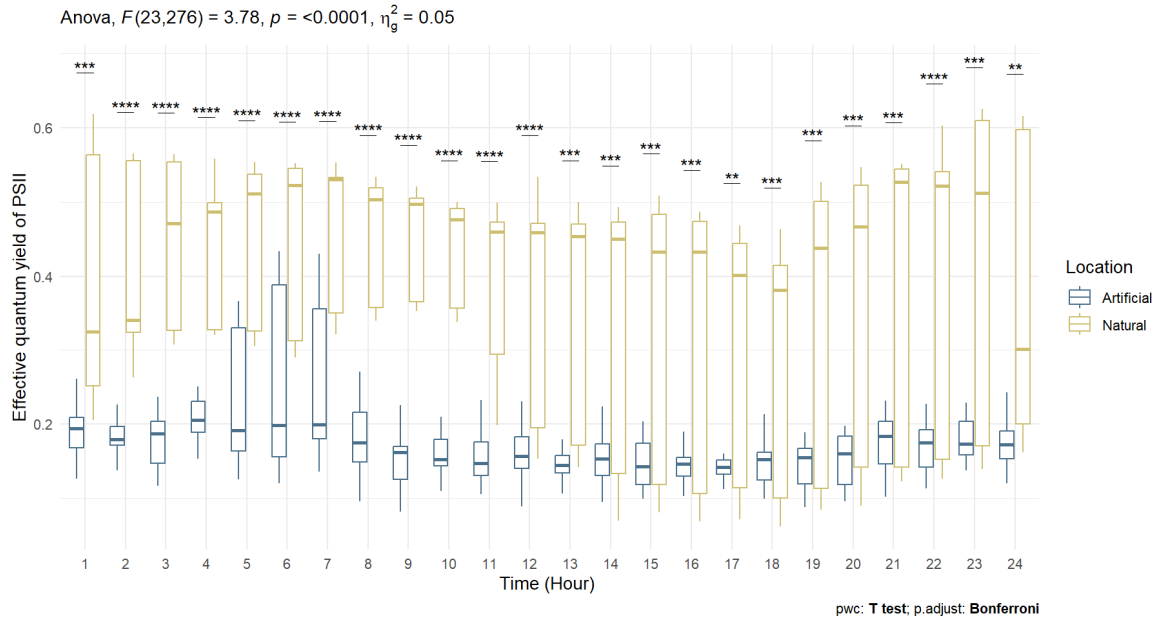

Figure 8*:* Change in Y(II) over hours in both sites, the data shown are based on measurements collected over three days in each site, labelled in blue is represented the artificial site and green the natural site. Calculations are based on three days measurements in each site, for a total of 830 replicates per each hour in each site. As a test to assess the statistical significance of the data, A two-way repeated measures ANOVA test was performed (results on the top of the graph). p-values, reported as follows: * = p-value < 0.05, ** = p-value < 0.01, *** = p-value < 0.001.

Y(II) change depending on the hour and depending on the site considered ((Fig 8). When considering both locations, data collected in the natural have higher Y(II) than data collected in the artificial site at each hour measured. However, the two site differ in the Y(II) measurement peak, in the natural site the highest Y(II) is found between 22:00 and 07:00. On the other hand, the highest yield in the artificial site is observed between 05:00 and 07:00. A two A two-way repeated measures ANOVA test was conducted to assess the effect of the location on the Y(II). A statistically significant correlation was found between Location and time (F 23, 276) = 30.4, p < 0.0001. P-values were adjusted using the Bonferroni multiple test correction method. The effect of location was significant at every time point all the p-values < 0.005. However, it should be noted that the condition of normality regarding the data collected in the natural site were not met due to their large variation over time.

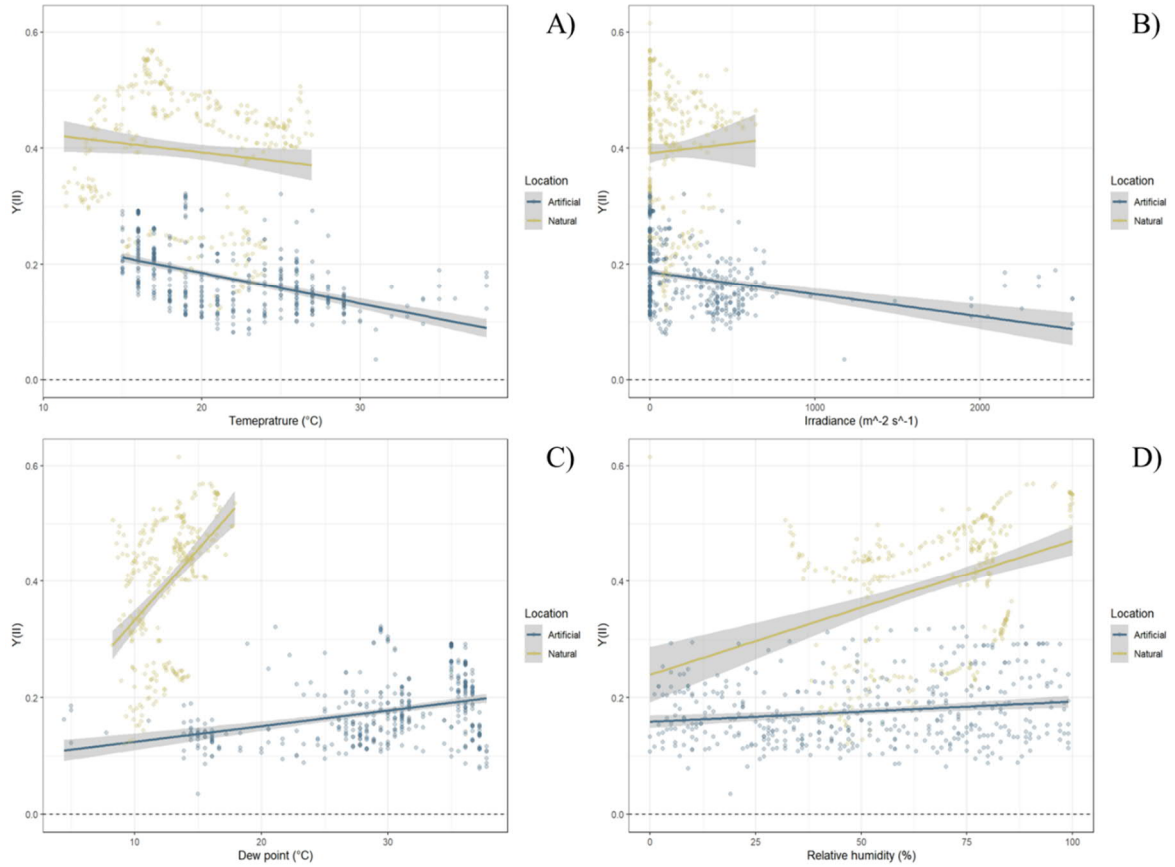

Figure 9: interaction effect of temperature (A), irradiance (B), dew point (C) and relative humidity (D) on the Y(II) in the measurement sites. Calculations are based on 730 observations over 3 days in each measurement site. In order to asses statistical differences a linear mixed effect model was fit. Data are based on the fitted values calculated within the model.

Interaction between environmental parameter and their effect on the Y(II) was calculated (Fig 9). Tendentially to an increase of the temperature, Y(II) tends to decrease (Fig 9A) in both, the artificial and in the natural site. The effect is rather noticeable in the artificial site, where the temperatures measured where higher, thus it has a higher negative impact on the Y(II) especially when temperature surpasses around 30 (°C), indeed it is possible to observe a sharp decrease of the Y(II). When considering, irradiance the pattern differ in the two sites, indeed to an increase of irradiance correspond a increase in Y(II) in the natural site, in the artificial site, when irradiance was too strong (over around 1000 µmol photons m^{-2} s^{-1}), the Y(II) decreased considerably (Fig 9B). Dew point and Y(II) are positively correlated in both the measurement sites (Fig 9C) Especially in the natural site it is noticeable that to an increase of the dew point correspond an increase of the Y(II) and, although not as strong, it is possible to observe the same relation in the artificial site as well. Relative humidity (Fig 9D) has a positive impact on Y(II) in both the measurement sites. The effect is more accentuated on the natural site and milder on the artificial. In fig 9D it is also noticeable the presence, of higher relative humidity measurements in the natural site rather than in the artificial site.

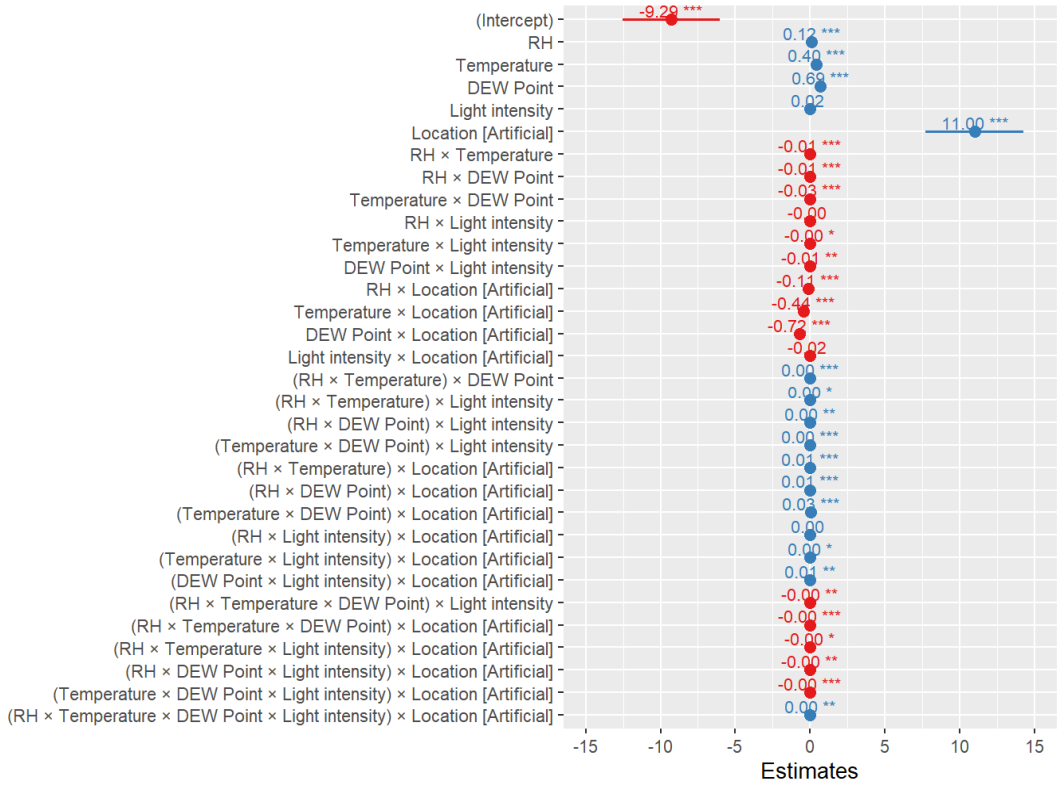

Figure 10: interaction effect between environmental parameters on the Y(II) in the two measurement sites. On the x axis are displayed the estimates, on the y axis the interactions between the fixed effects. On top of each line there are displayed the estimates values, the length of the line is based on the standard error, the colour is labelled as followed: red for negative estimates and blue for positive estimates. Moreover, on top of every line are displayed the p-values, labelled as follows: * = p-value < 0.05, ** = p-value < 0.01, *** = p-value < 0.001.

In order to assess statistical differences a LMM was fit, The model statics in Fig 10 are followings: AIC (-1108.742), BIC (-945.0066), log likelihood (590.3712) and DF = 696. In order to fit the model, Y(II) was set as dependent variable, as independent variable, the interaction effect between temperature, relative humidity, dew point and irradiance in the two locations was considered, day was set as random variable. The statistical calculations of the model were made considering the natural site as the reference site, on which the artificial site was tested against. All the interactions tested, are highly statistically significant (p-value<0.001). The intercept value is of -9.29, indicating the expected Y(II) when all the predictor variable (relative humidity, temperature, dew point and irradiance) are equal to 0 in the reference location (natural). The fixed effect of RH gives a positive estimate of 0.12, temperature 0.40, dew point 0.69 and light intensity 0.02. Indicating the increase of Y(II) per each variable, when all the other variables remain constant. When looking at the estimate in the artificial location, the estimates give a positive estimate of 11.00, indicating that the Y(II) in the artificial location is 11units higher than in the natural location, when all the variables are 0. Indicating the strong effect of the variables tested on the Y(II). When considering the two way interactions (artificial location x variable) show the following estimates: RH (-0.11), temperature (-0.44), dew point (-0.72) and light intensity (-0.02). Therefore, all the estimates

are negative and highly insignificant. The data explain that the variable tested on the artificial location have a negative impact on the Y(II). Three and four ways interactions, are mostly close to 0, indicating very small change in the Y(II) when their interaction is considered.

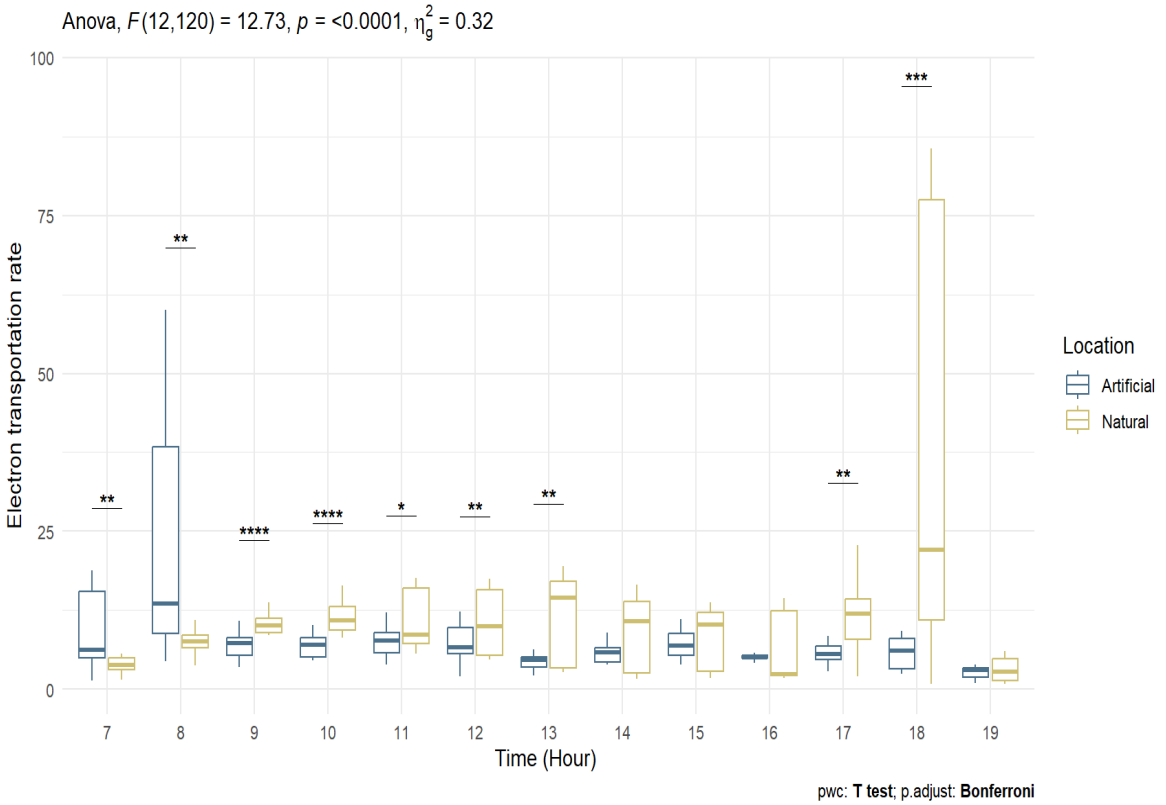

Figure 11: change of ETR over hours, in the 2 locations. Data are based on 422 replicates, over three measurement days. Data displayed are based on the estimated marginal means, error bars on top of the bars represent lower and upper CL. In order to asses statistical differences a two-way repeated measure ANOVA was conducted. p-values, reported as follows: * = p-value < 0.05, ** = p-value < 0.01, *** = p-value < 0.001. In the figure data regarding observation performed before 07:00 and after 19:00 are not included, due to no incident light reaching the algae, therefore the ETR was 0. The data were discarded in order to meet the ANOVA assumption.

According to the observation (Fig 11), ETR shows important differences between locations and hours. Measurements performed in the natural location display a higher ETR than in the natural location, during most of the hours. The only hours in which a higher ETR is observed to be higher in the artificial site, is at 7:00 and 8:00 therefore, in the morning. ETR in the natural location is the highest at 18:00 where the measurements show a sudden from 17:00 to 18:00, to then decrease the next hour at 19:00. On the other hand, in the artificial site the highest peak in ETR is reached at 7:00 and 8:00, hence showing a different pattern with the measurements collected in the natural site. In order to asses statistical differences a two-way repeated measure ANOVA test was conducted in order to asses the effect of location on the ETR over hours. Statistically significant interactions were found between Location and time on ETR F(12,20) = 12.73, p-value < 0.0001. Therefore, the effect of Location on ETR was analysed at each time point displayed. P-values were adjusted using the Bonferroni multiple testing correction method. The effect of Location was significant at every hour of the day, except at hour: 14, 15, 16 and 19. Additionally, pairwise comparison test shows that mean ETR was significantly

different between artificial and natural location and every time point (p-values < 0.005). However, it should be noted that the condition of normality regarding the data collected in the natural site were not met due to their large variation over time.

Laboratory experiment

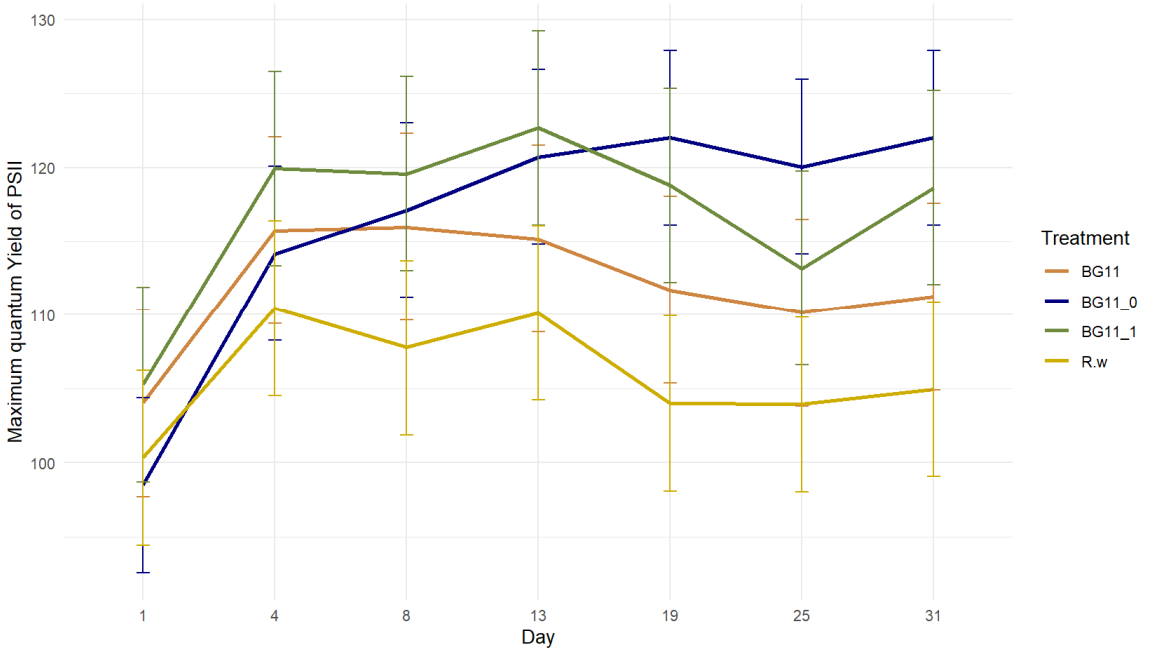

Figure 12: Change In Φmax PSII over time labelled by treatment. Calculations are based on 320 observations, for each treatment 5 replicates were prepared and a total of five measurement per each treatment each day were performed. In order to asses statistical differences a linear mixed effect model was fit. Data shown in the figure are based on the estimated marginal means obtained with the model, the error bar graphs represent the lower and upper CL

Treatment over time have different impact on the Φmax PSII. cultures treated with BG11_1 (labelled with green) present higher Φmax PSII every day, except on day 25, whereas cultures treated with BG11_0 have higher Φmax PSII. On the other hand, cultures treated with R.w (labelled with yellow) show the lowest Φmax PSII. When considering cultures treated with BG11_1 it is possible to see the highest increase of Φmax PSII since the first day, the Φmax PSII continues then increasing till day 13 to then decreasing till day 25 and then increasing again. Perhaps showing the tendency to increase furtherly. Most notably, cultures treated with BG11_0 show higher Φmax PSII when compared to cultures treated with BG11 and R.w.

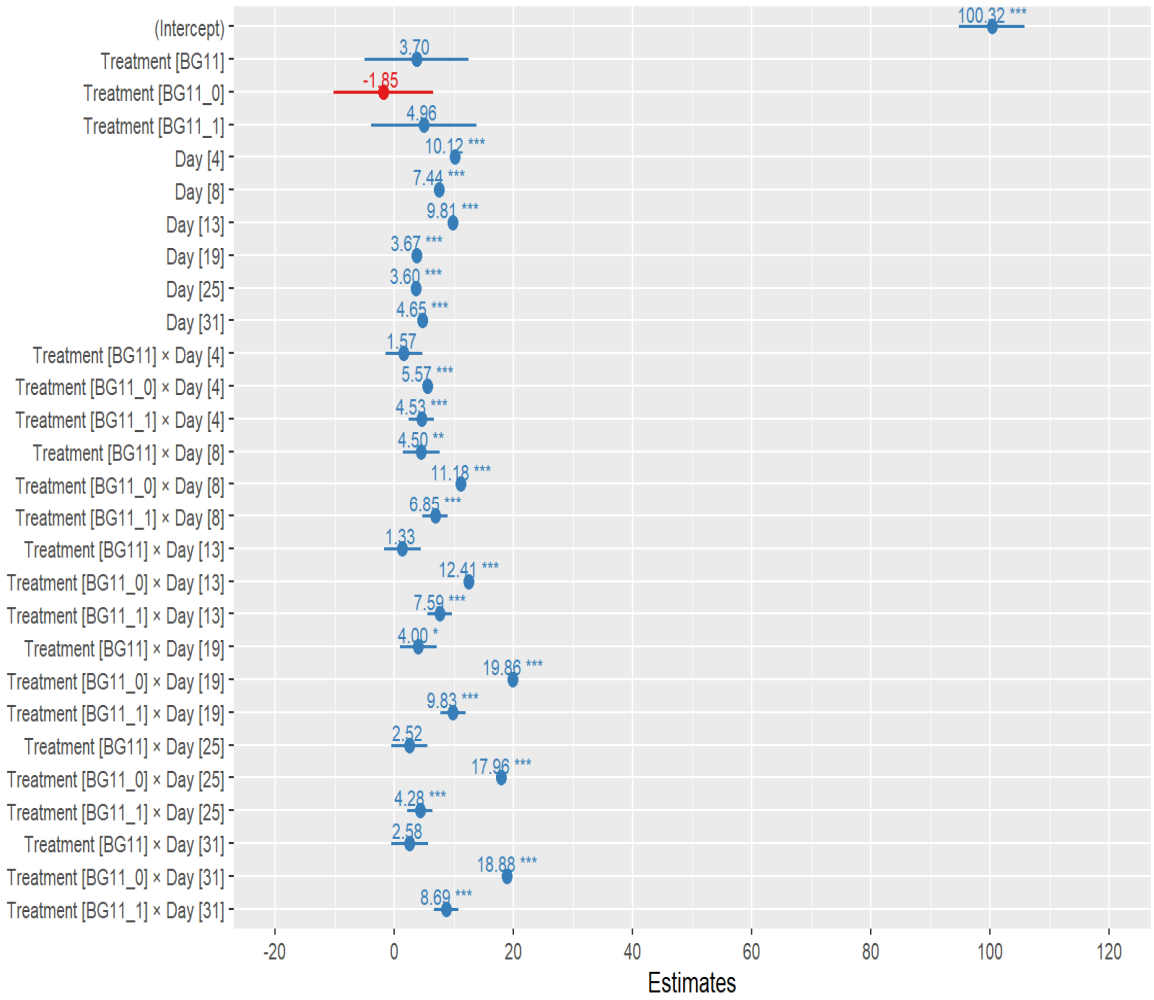

Figure 11: model statistics of Φmax PSII change over time depending on the treatment. In the figure estimates are displayed on the x axis, the fixed effects and their interactions on the y axis. In the figure are displayed the values of the estimates on top of each line and the p-values as follows: * = p-value < 0.05, ** = p-value < 0.01, *** = p-value < 0.001. the length of the lines represents, the standard error, the colour blue represents positive estimates, red shows negative estimates

In order to asses statistical differences a linear mixed effect model was fit, considering Day and treatment (Day *treatment) as fixed effect and the sample ID as random effect (1 | ID_sample). model statistics are the following: AIC (820.9894), BIC (909.2387) and Log likelihood: -380.4947 (df=30), the treatment R.w was used as reference treatment; therefore, its baseline level is labelled as intercept. The intercept estimate is 100.32 unites, being highly significant (p-value<0.01). When looking at the effect of the treatment alone on the Φmax PSII, there are no statistically significant differences, although the estimates are all positive except for cultures treated with BG11_0, showing a negative impact on the Φmax PSII. Moreover, when looking at the effect of the day alone on the Φmax PSII, all the estimates are positive and highly significant, showing a positive impact on the Φmax PSII over time. However, when considering the effect of the treatment combined with days on the Φmax PSII, all the estimates for every treatment are positive and highly significant, except for: BG11 x Day 4, BG11 x Day 13 and BG11 x Day 31, being the only ones not statistically significant. Treatments BG11_0 and

BG11_1 beside showing the highest estimate, and therefore the highest positive impact on Φmax PSII are all highly significant at each time point tested. The highest estimate registered are: BG11_0 x Day19, BG11_0 x Day25 , BG11_0 x Day 31 and BG11_1 x Day19. The following model and statistical calculation explain that the treatments alone do not have statistically significant effect on the Φmax PSII. However, when the effect of the treatments is combined with the day, almost all the interaction are highly statistically significant, especially for the treatments BG11_0 and BG11_1, confirming the presence of highly statistical differences among treatments over the days.

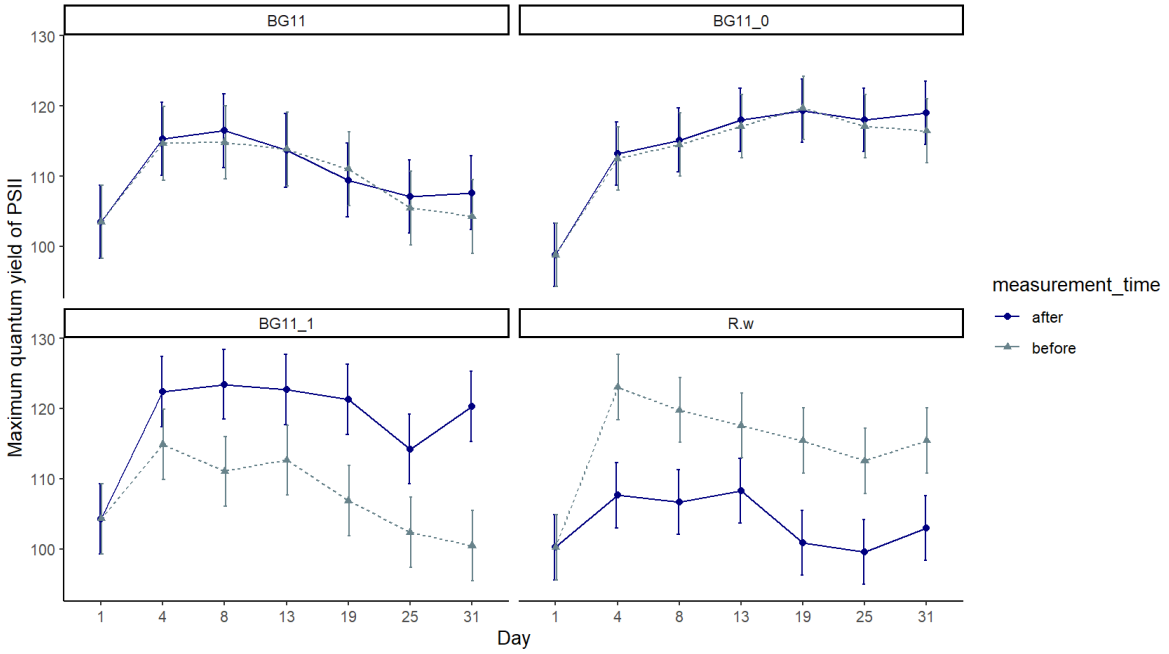

Figure 14: Difference between Φmax PSII before and after providing the treatments over days. The figure is organized in 4 different line plots, each representing one treatment (title indicating the treatment above). Data are based on 640 observations (320 measurements performed before and 320 after providing the treatments). In the line plots there are bar lines representing the upper and lower CL of the estimated marginal means. In order to asses statistical differences a linear mixed effect model (LMM) was fit

In figure 14 are represented the differences between before and after providing the treatments on the Φmax PSII in the 4 different treatments tested. When looking at cultures treated with BG11_1, it is possible to observe the tendency of the Φmax PSII to be higher directly after providing the treatments, indeed already after the first day, measurements diverge, showing a considerably higher Φmax PSII directly after having provided the treatments. However, data collected from treatments BG11_0 and BG11 displays no differences between the measurement time, cultures treated with these two treatments displays little or no differences. Moreover, cultures treated with R.w show the opposite trend where Φmax PSII is higher before providing the treatments.

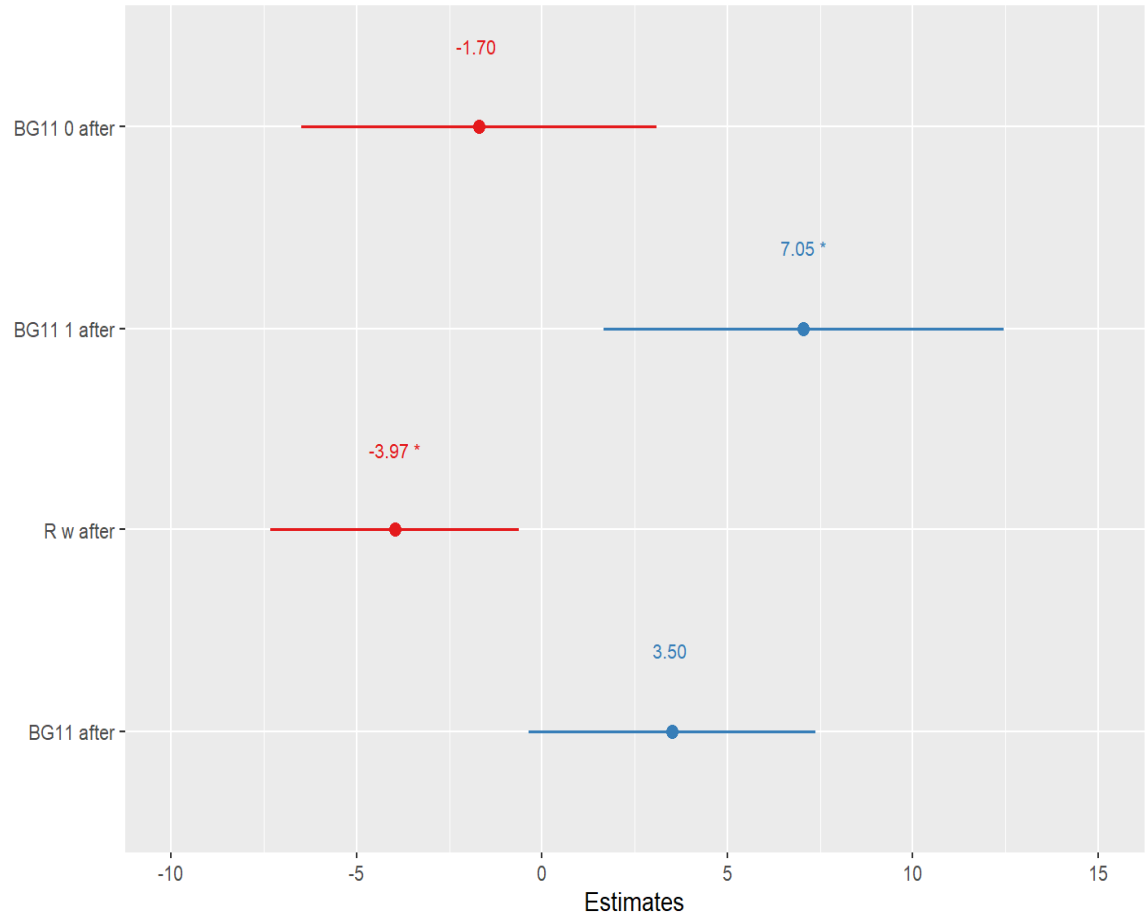

Figure 15: Model displaying statistical differences of the Φmax PSII after having sprayed the treatments. On the x axis are displayed the estimates and on the y axis is displayed the treatments after having provided the treatments. In the plot, line length represents the standard error, the colour blue represents positive estimates, red shows negative estimates. In the figure are displayed the values of the estimates on top of each line and the p-values as follows: * = p-value < 0.05, ** = p-value < 0.01, *** = p-value < 0.001.

In order to asses statistical differences a LMM was fit, the model statistics are the followings: AIC (1740.266), BIC (1936.337), log likelihood (-814.1332), df = 226. After having sprayed the treatments BG11_0 and R.w display the tendency to have a slightly lower Φmax PSII**,** However the results being not statistical significant for BG11_0 and being statistically significant for R.w. Cultures treated with BG11_1 have a considerably higher Φmax PSII after having provided the treatment (estimate = 7.05), with the result being statistically significant. Furthermore, cultures treated with BG11 display higher Φmax PSII after having sprayed the treatments, with the result being not statistically significant.

Morphological changes in the course of different treatments

	BG11	BG11-0	BG11-1	R.w
Day 1				
Day 8				
Day 16				
Day 24				
Day 31				

Table 2: change of *Trentepohlia aurea* over the days 1, 8, 16, 24 and 31, columns are divided by treatments and row per observation day.

Trentepohlia aurea experienced some morphological changes over the days, which is already recognized with the bare eye (Table 2). Samples treated with BG11 starting from the day 16 were observed to develop colonies of *Anabaena sp* (greenish material surrounding the sample upon the substrate). Moreover, samples treated with BG11-0 darkened over time. Finally, when looking at samples treated with BG11_0, BG11_1 it is possible to see some reddish material surrounding the algae on the substate. The reddish material found were carotenoids accumulation.

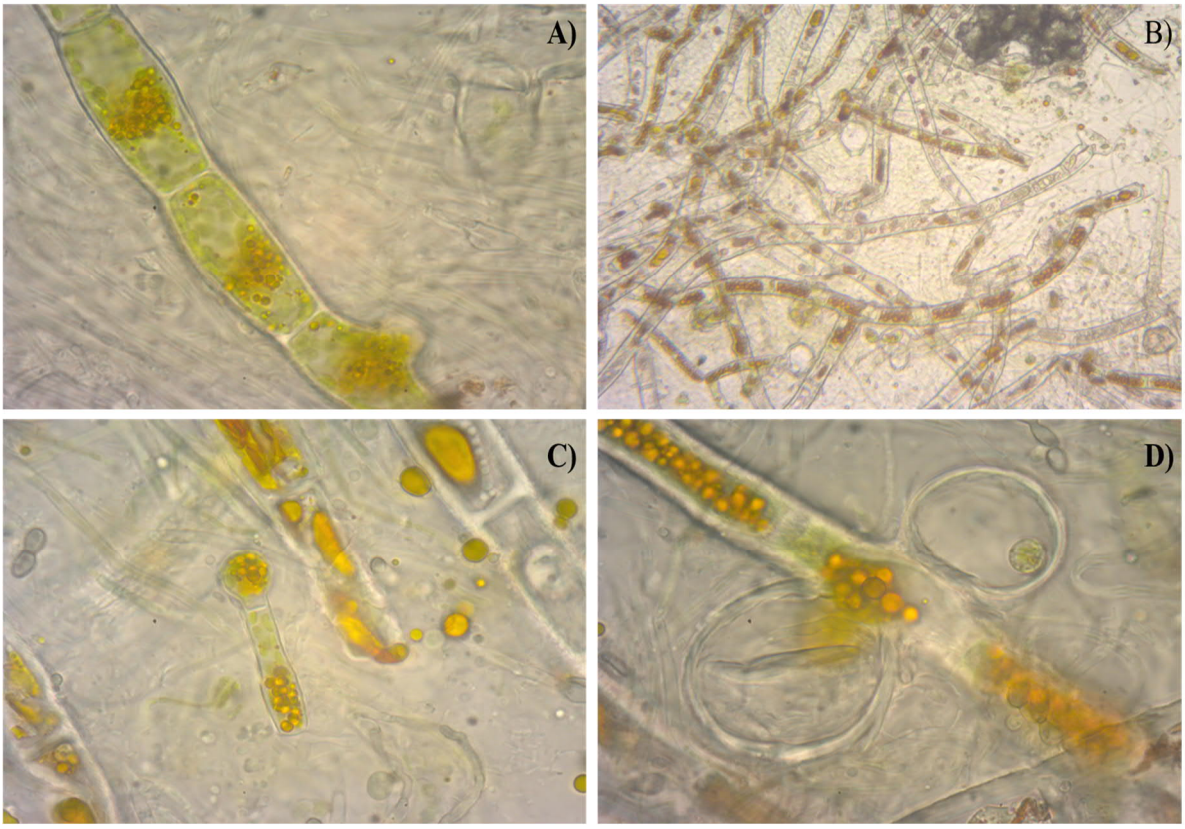

Figure 16: sections of *Trentepohlia aurea* cells treated with BG11, images obtained with light microscopy.

In figure 16 are shown sections of *Trentepohlia aurea* cells treated with BG11. At the end of the experiment, sections of *Trentepohlia aurea* were analysed with light microscopy, in order to asses whether or not there were structural differences among treatments. In Fig 16A are represented chloroplast within cells, in fig 16B are shown several cells in an unhealthy condition. Fig 16C and 16D show respectively a spore and a sporangia. Indeed, in cultures treated with BG11, several spores and sporangia were found.

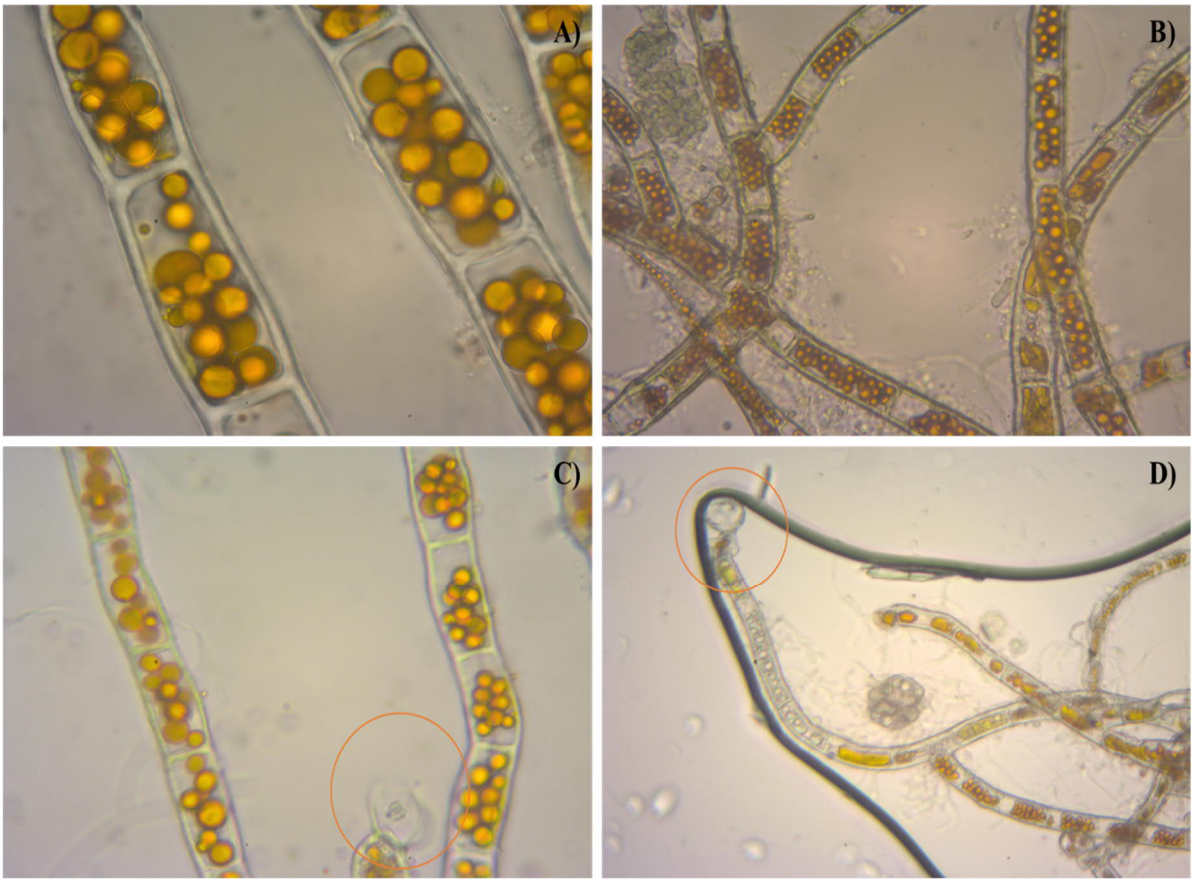

Figure 17: sections of *Trentepohlia aurea* cells treated with BG11_0 (BG11 nitrogen depleted), images obtained with light microscopy.

In figure 17 are shown sections of *Trentepohlia aurea* cells treated with BG11_0. A detail that is also notably visible in the images, is that cells treated with BG11_0 seem to have a larger number of carotenoid vesicles within their cells. Hence, Fig 17A, B and C appear to display cells with big number of carotenoids within their cellular space. Together with large number of carotenoids, when inspecting cultures treated with BG11_0 were also found different gametangia, visible in Fig 17C and D, underlined by a red circle.

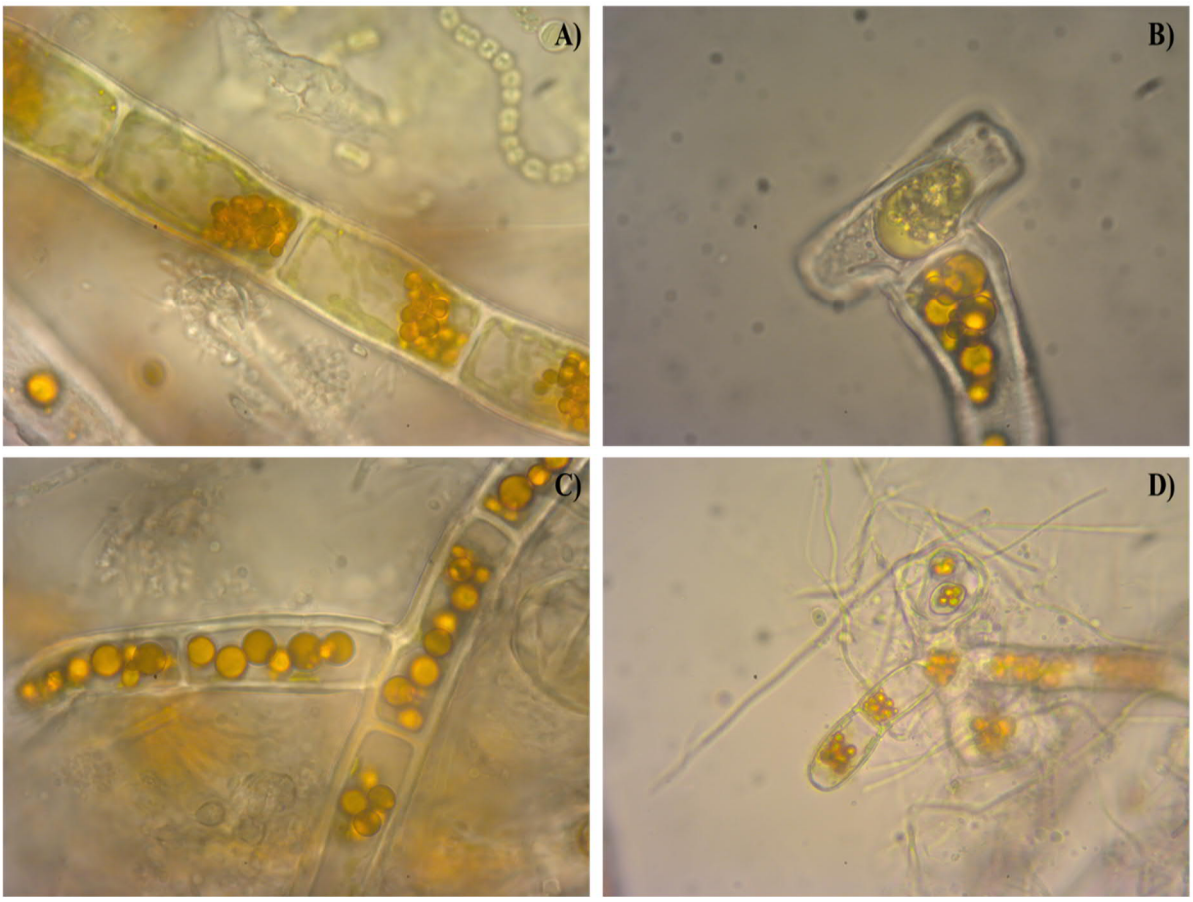

Figure 18: sections of *Trentepohlia aurea* cells treated with BG11_1, images obtained with light microscopy.

As displayed in Fig 18, different new cells formation structures were found when analysing cultures treated with BG11_1. In Fig 18A is possible to see colonies of *nostoc* in the sample. Furthermore, in cultures treated with BG11_1 it was possible to visualize different structures suggesting new cells formation (Fig 18B). Moreover, different gametangia structure (Fig 18D) were found, when considering carotenoids production within cells it seems that cultures treated with BG11_1 have more carotenoids than cultures treated with BG11 but less than BG11_0.

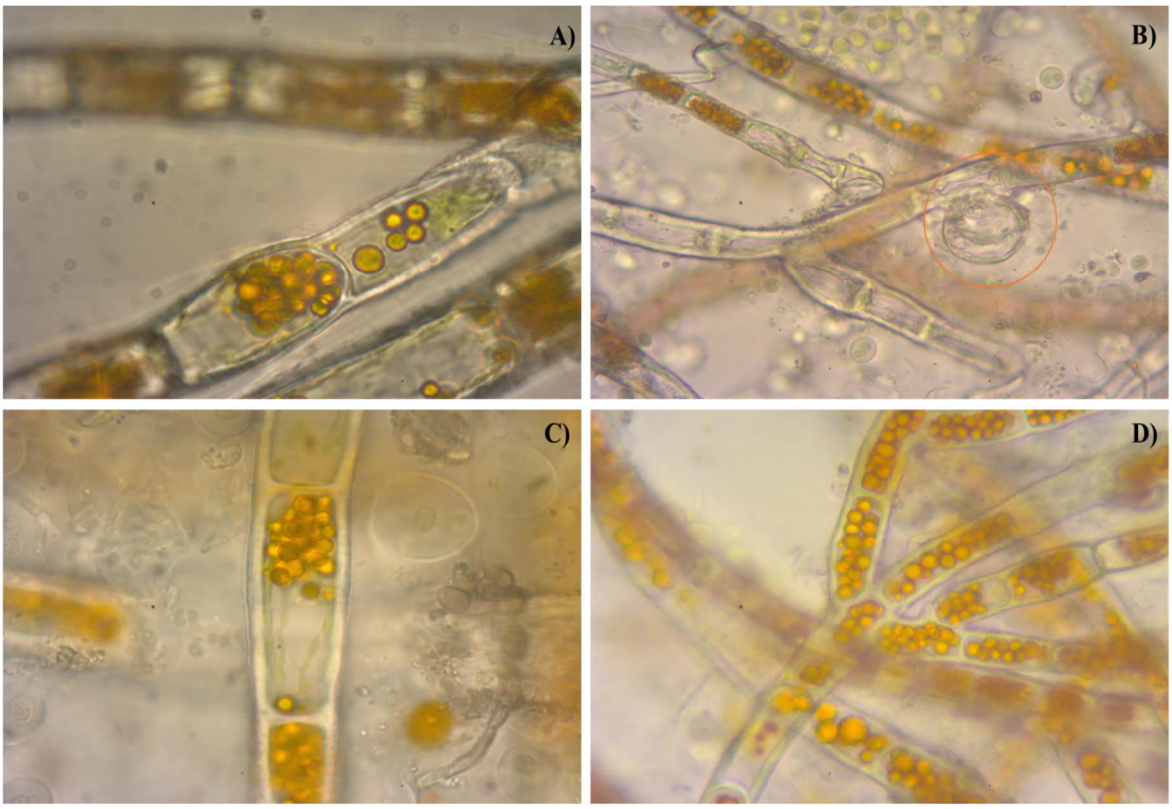

Figure 19: sections of *Trentepohlia aurea* cells treated with R.w (rainwater), images obtained with light microscopy.

Lastly cellular structures in cultures treated with rainwater (R.w) were inspected (Fig 19). Cultures treated with rainwater, alongside cultures treated with BG11_0 appeared to present high amount of carotenoids within their cells (Fig 19D). During the inspection different sporangia structures were found (Fig 19B).

Estimation of total carotenoids volume and size

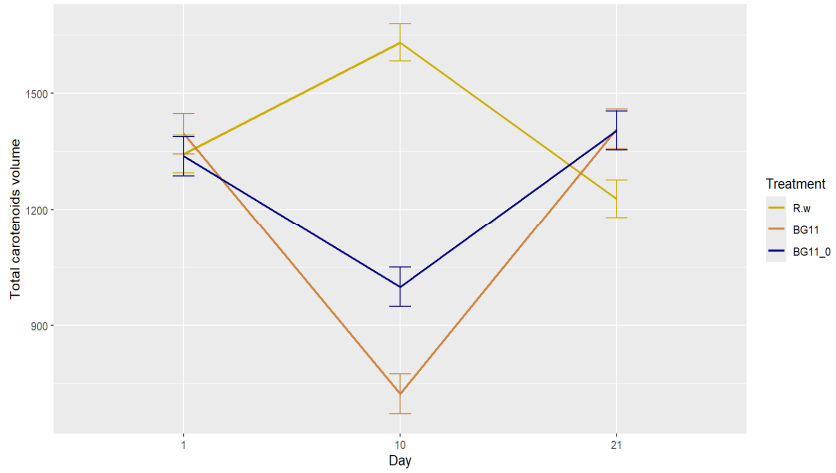

Figure 20: Estimation of total carotenoids volume over time. three replicates per each treatment, each observation day were analysed for a total of 27 replicates. In order to assess statistical difference a linear mixed effect model was fit. Values in the figures are based on estimated marginal means, error bars indicate upper and lower CL.

Total carotenoids volume was estimated (Fig 20). Carotenoids volume differ within cells according to the treatment. When the algae are treated with BG11 and BG11_0, already on the 10th observation day there seems to be a decrease in total carotenoids volume, to then increase on the 21st day, and both reaching similar values. On the other hand, cultures treated with R.w display the opposite tendency, whereas on the 10th observation day, total carotenoids volume is higher, to then slightly decrease on the last observation day.

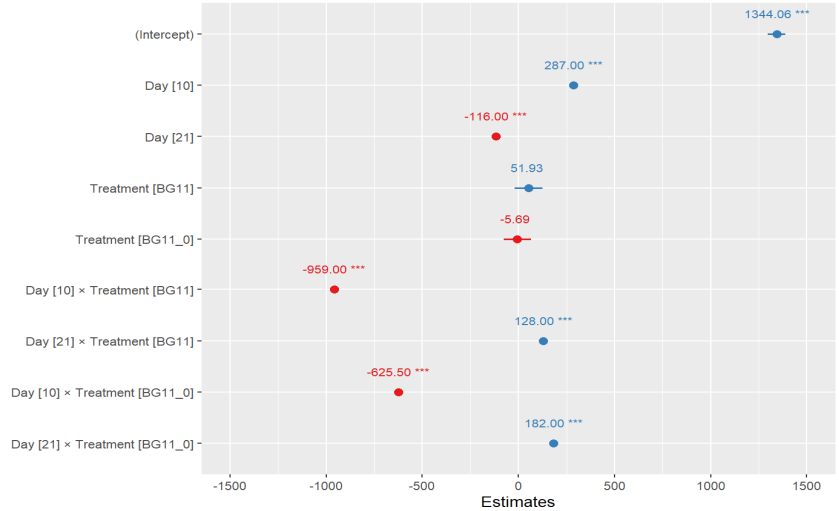

Figure 21: linear mixed effect model displaying statistics relative to total carotenoids volume change over time by treatment. Fixed effect interactions are displayed on y axis, estimates are on the x axis. The exact values of the estimates are written on the dots, the line length display the standard error. Statistically significant difference of each interaction are displayed as follows: * = p-value < 0.05, ** = p-value < 0.01, *** = p-value < 0.001.

Statistical differences were assessed with the linear mixed model displayed in figure 21. The model specification are the followings: AIC (294.9981), BIC (311.9152), log likelihood (-128.4991) and df = (6-12). Treatments BG11 and BG11_0 were tested against the referment treatment R.w. Estimated on the day effect alone are positive on day 10 and negative on day 21st being highly statistically significant (p-value < 0.001), on he other hand if the effect of the treatments is considered alone, estimates are not statically significant, with BG11 treatment having the tendency to increase total carotenoids volume and BG11_0 decreasing it. However, when considering the interaction effect of the treatments over time (Treatment x Day) all the interactions are highly statistically significant (p-value < 0.001). Both BG11 and BG11_0 decrease the total carotenoids volume on the 10th measurement day, with BG11 having the higher negative impact, however on the 21st day, both BG11 and BG11_0 increase the total carotenoids volume, with BG11_0 displaying the highest increase with the estimates at 182.00.

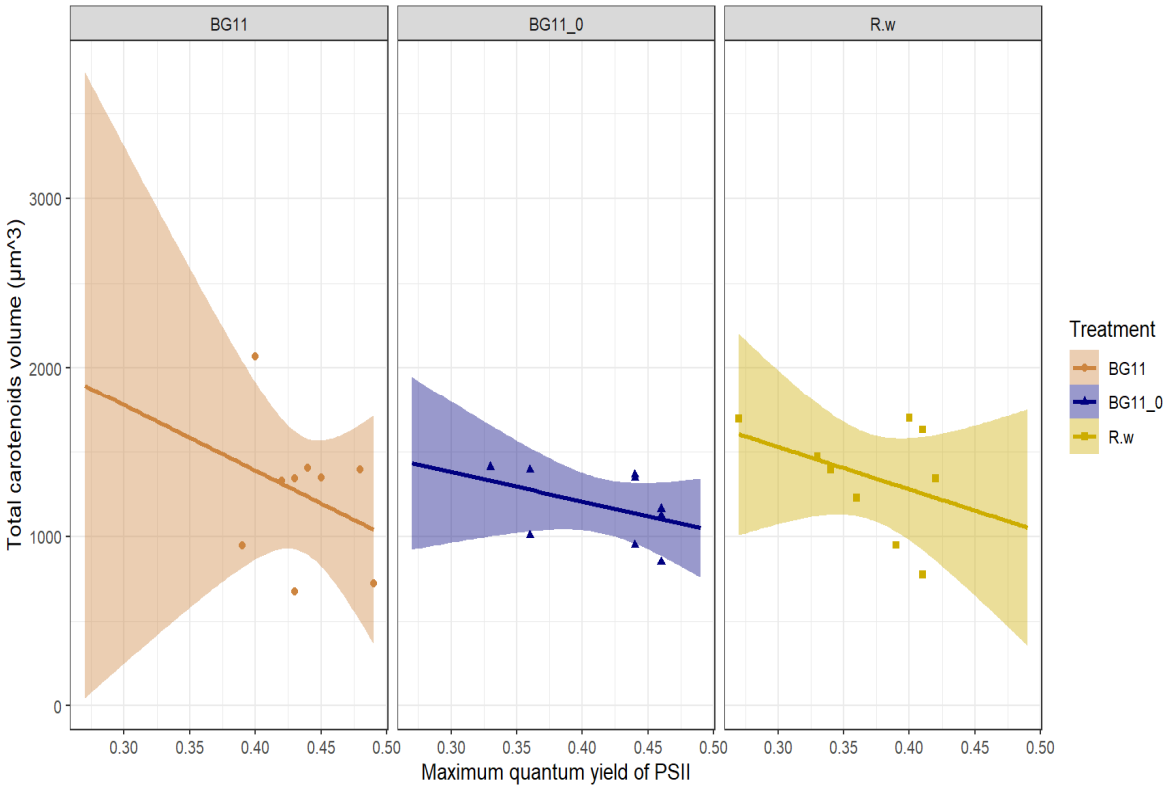

Figure 22: relation between total carotenoids volume and Φmax PSII grouped by treatments. BG11, BG11_0 and R.w. For each treatment, the confidence interval around each regression line is shown as coloured area.

The relation between Φmax PSII is represented in figure 22. Both, cultures tested with BG11, BG11-0 and rainwater show similar trend, it is noticeable the tendency that the higher the Φmax, the lower the total carotenoids volume.

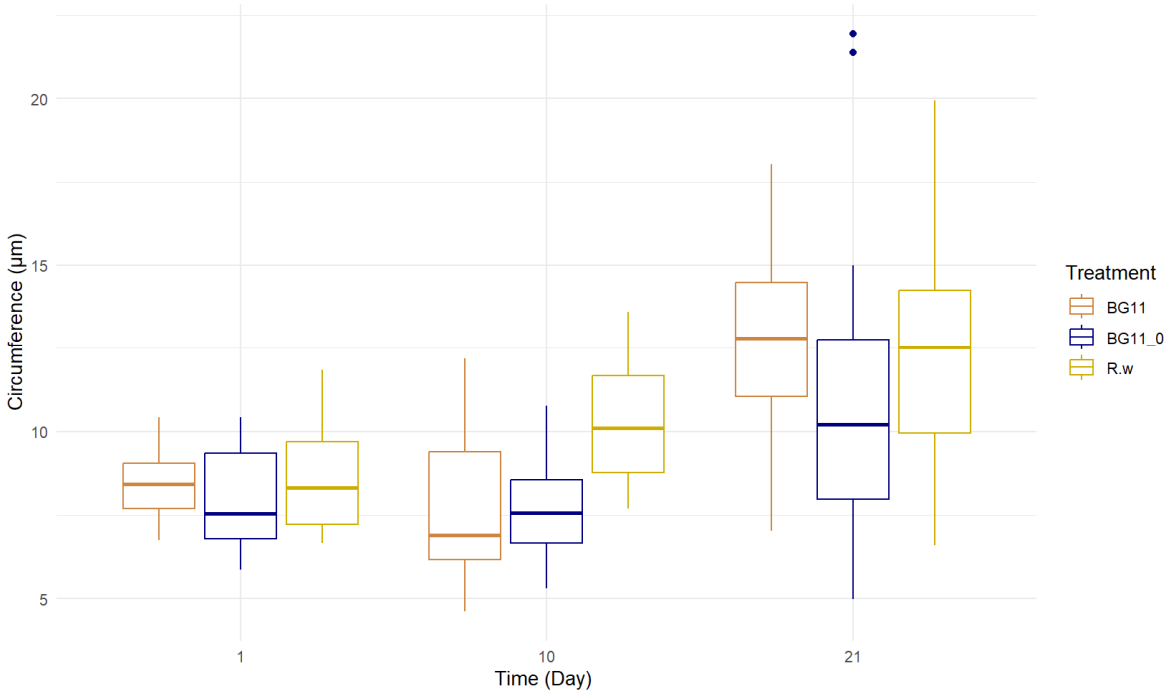

Figure 23: carotenoids vesicle size measurements. Data are collected in three different measurement time (on the first, tenth and twenty first day of the observation period). For each day a total of three cells were analysed, for each cell 10 vesicles were measured for a total of 30 replicates per each treatment each measurement day. In order to asses statistical differences a two-way repeated measure ANOVA was conducted.

Carotenoids vesicles size were measured (Fig 23). On the 10th measurement day there is the tendency for cultures treated with R.w to display higher vesicle size when compared to cultures treated with BG11 and BG11_0. Moreover, overall, when considering the quartile range, cultures treated with BG11 show a higher size than cultures treated with BG11_0. However, if considering the median, cultures treated with BG11_0 display higher vesicle size. On the 21st measurement day carotenoids vescicle size have increase in all the treatments tested. Furthermore, cultures treated with BG11 and R.w, tendentially lead to higher carotenoids vesicle size. A two-way repeated measure ANOVA was performed to evaluate the effect of treatment, at each time point on circumference. There was no statistical difference between treatment and time on circumference $F(1,19) = 0.817$, p-value > 0.05. However statistically significant differences were found when considering time alone (change in circumference size, without considering treatments). $F(2,14) = 23.700$, p-value < 0.05. P-values were adjusted using the Bonferroni multiple testing correction method.

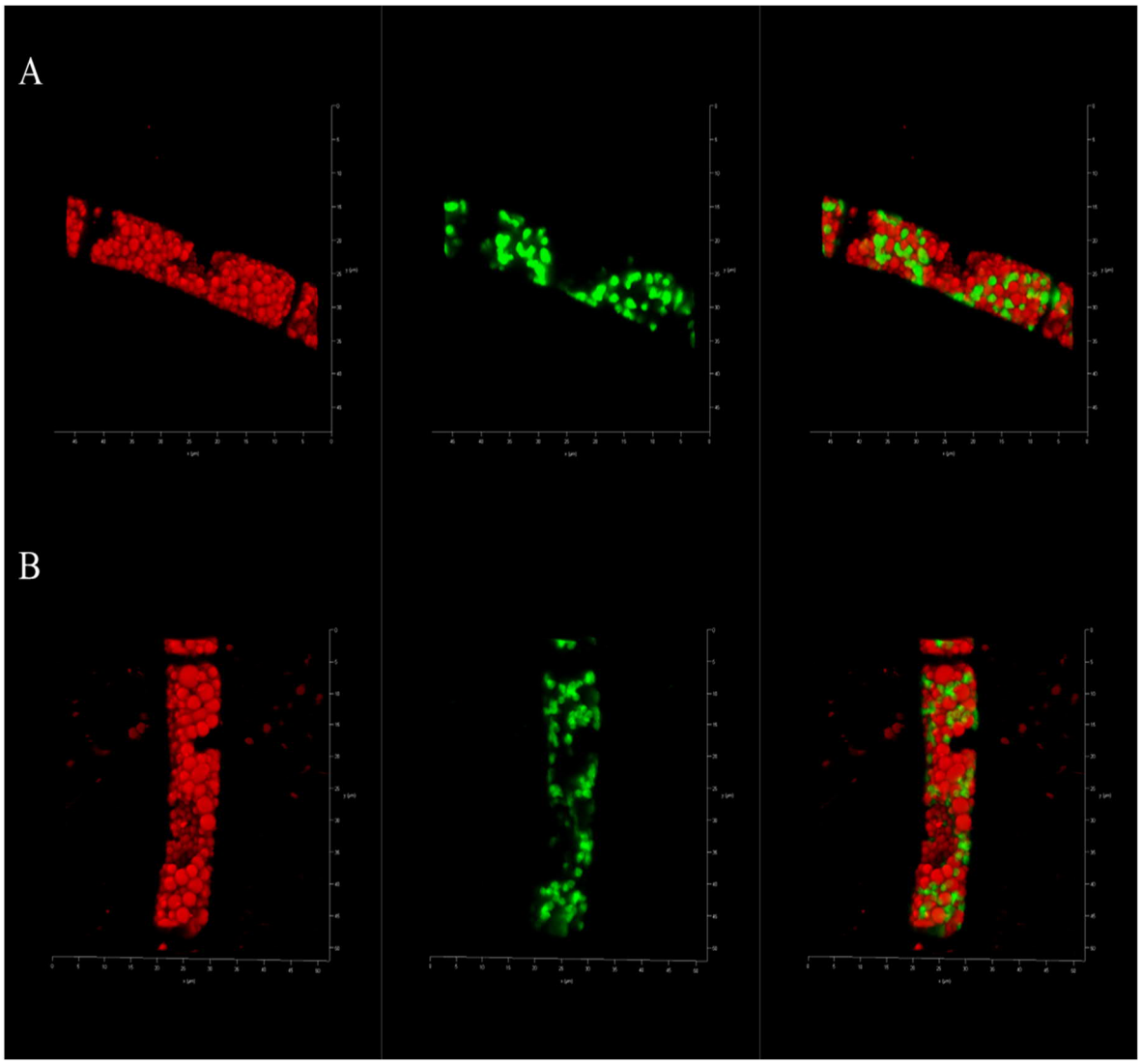

Figure 24: 3D reconstruction of two *Trentepohlia aurea* cells (A and B). the laser line 514 was set at a wavelength between 530 nm – 570 nm to detect the carotenoids fluorescence, the laser line 488 was set at a wavelength between 650 nm – 700 nm to detect chloroplasts fluorescence. Carotenoids are labelled in red, chloroplasts in green. Scale bars indicate size of cells.

Figure 24 was obtained with the CLSM software powered by Leica. It is obvious that carotenoids fill a large portion of the cellular volume, with chloroplasts hardly visible without autofluorescence.

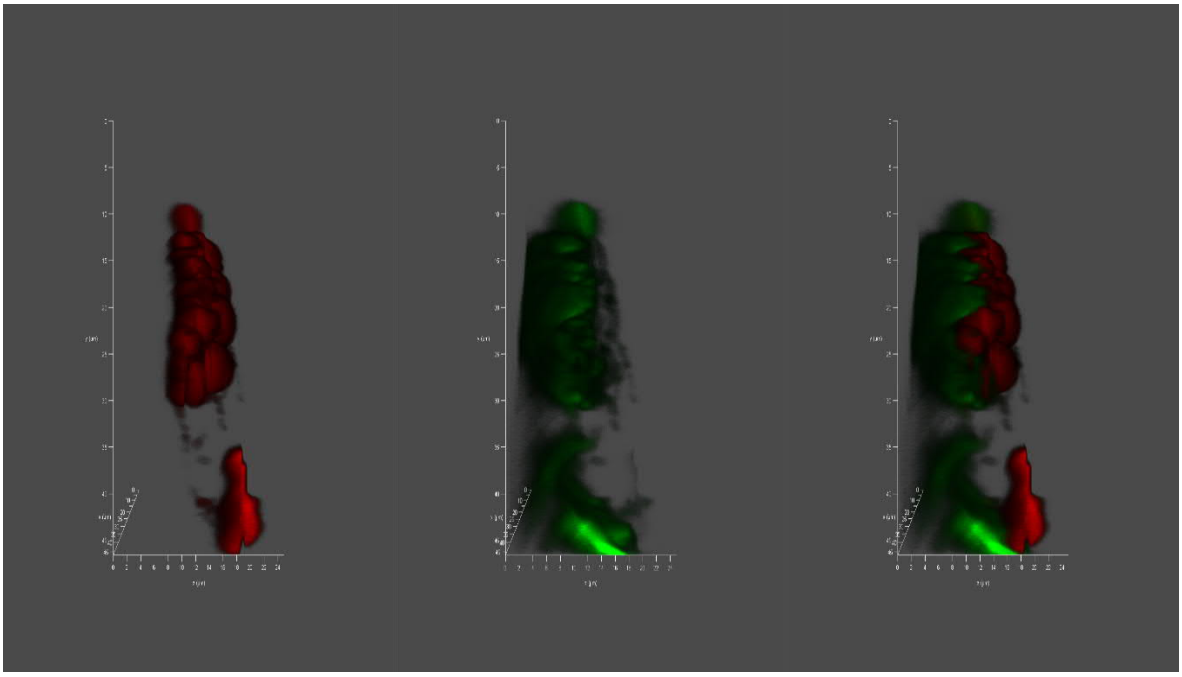

Figure 25: profile section of a *Trentepohlia aurea* cell with scale bar. The laser line 514 was set at a wavelength between 530 nm – 570 nm to detect the carotenoids fluorescence, the laser line 488 was set at a wavelength between 650 nm – 700 nm to detect the chloroplasts fluorescence

In Fig 25 is represented a longitudinal section of a cell of *Trentepohlia aurea*. Detection information is specified in the figure description. It seems that chloroplasts (labelled in green) are positioned mainly beneath the carotenoids surface (labelled in red). When looking at the profile section of the cell it seems that chloroplast have a cage like structure, twined around the carotenoids

Discussion and conclusion

Environmental parameters and effective quantum yield of PSII. Differences in environmental parameters were assessed in order to characterize differences between the natural and artificial site. As stated in the material and methods paragraph, the natural site appeared to be a healthier site for *Trentepohlia aurea*. Healthy, reddish coloured tufts were covering the limestone substrate suggesting optimal growth condition. Algae colonies on the artificial site were small and less spread on the wall; the species was barely present in small spots thus indicating the less favourable habitat. When considering temperature (Fig 7A) the artificial site shows in general higher measurements especially at 18:00, reflecting the location, fully exposed to the sun, lacking any vegetation cover, being shadowed only during nocturnal hours. On the other hand in the natural site temperature seems to be considerably lower, which is probably due to the vegetation cover acting as a barrier against incident light and therefore decreasing temperatures. Indeed generally dominance of Trentepohliales members are found in open space with low temperatures (Kharkongor and Ramanujam 2014). Assessing optimal temperature parameters for *Trentepohlia aurea* is important also when considering carotenoids

production. *Trentepohlia aurea* carotenoids production was higher at low temperature (abe et al. 1998). Light intensity (Fig 7B) was measured in both the artificial and natural site, measurements are similar across the two sites, with the natural site having lower incident light reaching the algae. Kharkongor and Ramanujam (2014) reported that most of *Trentepohlia* specie thrive in environment with low light intensity, (Saraphol et al. 2020) found that the majority of species of the genera *Trentepohlia* were found during winter season at low air temperature and light supply, creating better growth conditions for the algae. Furthermore, information regarding light intensity on the algae are of importance in the context of carotenoids production. Abe et al. (1998) reported increased carotenoid production when *Trentepohlia aurea* is exposed to high light. Relative humidity (Fig 7C) is considerably different across the two sites. Hence in the natural site relative humidity follows a curved pattern, with higher measurements in the morning and over night reaching the highest peak at 5:00 with over 80 % of relative humidity to then decrease over the warmer hours of the day in the afternoon. In the artificial site, relative humidity is characterized by many ups and down all over the day probably due to the location characteristics. As the location being a parking slot without vegetal or artificial cover, therefore being fully exposed to wind currents. Early in the morning and over night it seems to present slightly higher values, reaching a maximum of almost 70 %. Indeed high relative humidity is an important environmental factor promoting high growth in species of the genera *Trentepohlia,* which is in agreement to our site comparison (Guiry and Guiry 2015, López-Bautista 2008, López-Bautista et al. 2002, Rindi 2007, Rindi et al. 2009). Dew point (Fig 7D) appears to look quite different across the two sites. Dew point in the natural site is much lower than compared in the artificial site. In the natural site, the dew point remains low all over the day meanwhile in the artificial site is much higher over 30 (°C) As shown in figure 8 and 11 Y(II) and ETR vary considerably between the two locations. In particular in the natural locations, Y(II) is higher at every hour of the day, moreover ETR displays the highest values over most of the hours considered. It should be note that although the two-way repetead measure ANOVA test were highly significant, the condition of data normality for data collected in the natural and for some hours in the artificial site was not respected, probably due to the considerably high number of measurements and to the environmental conditions which were rapidly changing. Furthermore, in Figure 9 interaction between environmental condition and location on the Y(II) show that environmental conditions in particular relative humidity and dew point have a positive effect on the Y(II), increasing it. On the other hand, temperature and light intensity, when too high, tend to decrease it, having a bad impact on the Y(II). Overall, the results display confirms out initial hypothesis, that *T.aurea* is in better condition in the natural site. This is due probably to the fact that environmental parameters, such as temperature, light intensity, relative humidity and in particular dew point have a better impact on the algae colonies in the natural site.

Maximum quantum yield of PSII vs treatments. In our present study *Trentepohlia aurea* was cultured in the laboratory with treatments containing different nitrogen concentrations. Φmax PSII was measured in order to assess overall growth and health condition of the algae and thus getting insight of what they may be the best conditions for the algae to increase carotenoids synthesis. Two different substrates were tested, agar at a concentration of 1,5% and marmolade in order to assess the best substrate to utilize. Samples cultured with agar agar died or showed signed of necrosis already after the first week, suggesting to not be suitable

for its utilization. On the other hand, samples treated with marmolade, (which was currently utilized for the whole experiment and displayed in the pictures in table 2) demonstrated to be suitable and optimal for the experiment as it may resemble the rocky substrate on which *T. aurea* grows in its natural environment. Cultures treated with BG11_0 and BG11_1 resulted in significantly higher Φmax PSII compared to cultures treated with BG11 and R.w (Fig. 12). Our observation indicate potential sensitivity against excess nitrogen supply. Nitrogen is an important compound in algae cellular pathways, nitrogen deficiency was shown to inhibit cellular division and synthesis of new protein within the cell. Furthermore, causing metabolic pathways to shift towards lipid synthesis due to the de novo production of triglycerides (Bellotti et al. 2013). Moreover, nitrogen deficiency lowers the level of chlorophyll a and increase the number of carotenoids (Geider et al. 1998). Although being an important compound in the overall cell health, *Chlorella vulgaris* and *Nannochlopsis* have shown to not be impacted by nitrogen deficiency and demonstrate the same growth rate of cultures enriched with full media, producing at the same time higher amount of lipids (Converti et al. 2009). Nitrite excess in concentrations over 5mg NL^{-1} showed inhibitory effect on a microalga – nitrifying bacteria culture dominated by *Chlorella* (Gonzalez-Camejo et al. 2020). Moreover *A. tomarense* showed negative correlations with excess of nitrate and growth performance (Shi et al. 2005). Furthermore, different other studies (Kızılkaya and Unal 2019, Hwang and Lu 2000) observed that excess of nitrate is harmful to phytoplankton growth and that the excess of nitrate significantly decrease Φmax PSII of *Chlorella vulgaris*. Nitrate can be stored by the cell as a nontoxic form of nitrogen (Tylova-Munzarova et al. 2005). However, nitrite, being an inorganic monovalent, impacts the photosynthetic process considerably (Spiller and Bögel 1977, Loranger and carpentier 1994). Indeed, photosynthetic electronic transport can modify intracellular pH, damaging cellular membrane(Almeida et al. 1995, Yang et al. 2004). Hence the increase of nitrate could have induced a decreased in growth and chlorophyll degradation (Chen et al. 2009). Which explain our observations. Another explanation however could be Na, which is provided as $NaNO_3$ and Na_2CO_3 in the BG11 medium utilized. Perhaps the amount of Na provided it was too great, leading to accumulation of Na, not being absorbed by the cell. Na in excess not being absorbed, it could have been deposited in the medium leading to its alkalinization and therefore impacting negatively on the growth performance of the cultures (Wang et al. 2019). Perhaps *T. aurea* is sensitive to Na, because Gupta and Agrawal (2002) observed that the species were not able to tolerate NaCl.

It should be noted that (Abe et al. 2003) cultured *T. aurea* with nitrate, nitrite and ammonium to study uptake of nitrogen during growth. Interestingly, in their study *T. aurea* demonstrated a higher removal rate of ammonium rather than with nitrate and nitrite. The preferred ammonium uptake can be explained by the more efficient of incorporation of already reduced nitrogen compounds into amino acids, which was already found in various other algae species such as *Chlamydomonas sp* where NH^+_4 was the source of N preferred with respect to NO_3 (Fernandez and Galvan 2007). Nitrate and nitrite first need to be reduced to amino groups, which is energy demanding and additionally requires reduction equivalents. Ammonium allows for a faster turnover of nitrogen into amino acid, leading to a greater protein production, instead, NO_3 was found to be responsible for a greater glutamate content, due to a lower turn out of glutamate into amino acids. (Lachmann et al. 2019), moreover NO3 in order to be utilized by the cells requires a higher energy demand in terms ATP (Ruan and Giordano 2017). However, because *T.aurea* occupies a narrow ecological niche in terrestrial environments, the study should be scrutinized as the author may misidentified the taxon.

Our findings showed that Φmax PSII was higher directly after treatments in cultures treated with BG11_1 (being statistically significant) and R.w, although data regarding R.w are statistically insignificant, a tendency can be seen (Fig 14). Higher Φmax PSII in cultures treated with BG11_1 after providing the treatments can be explained by the effect of nitrogen repletion after starvation. Treatments were provided via spraying on the cultures. Once sprayed, part of the treatment is deposited on the algae colony and therefore being absorbed for growth, while another part on the substrate, creates a thin water layer and therefore not being up taken. Once the treatment is sprayed again on the samples, the algae colony from a condition of nutrient stress, transit to a favourable nutrient condition. Perhaps the resupply of $NaNO_2$ and therefore of a N source could have lead to higher metabolic activity, as it was also observed in *T. mintus* (Gigova et al. 2015)

We performed also light microscopy inspections to characterize morphological differences between treatments. During the inspections, major differences were found in cultures treated with BG11_0 when compared to cultures treated with BG11 those cultures seemed to possess a higher content of carotenoids in their cells. Overall, cells formation structures such as cells in division stage and sporangia were found in all the cultures. Samples treated with BG11 generally showed signs of cell damage, and more death cells were found in respect to other treatments. A visual morphological evaluation of the samples was conducted (Table 2), cultures treated with BG11 were the only developing invasive contaminations with other organisms. Interestingly, orange spots were found surrounding the samples treated with BG11_0 and BG11_1, which it is also noticeable at naked eye (Table 2). Being unlikely these orange spots were carotenoids, they could have been *Trentepohlia aurea* propagations. In cultures treated with BG11_0 and in a smaller degree in cultures treated with BG11_1, but not in cultures treated with BG11 and RW. This could be due to the fact that cultures treated with BG11_0 were nitrogen depleted, therefore promoting a major carotenoids production, moreover samples treated with nitrogen depleted medium seem to darken over time (table 2). Abe et al 2007 observed that the green alga *Coelastrella striolata* would change colour from green to orange when cultured in nitrogen depleted media due to the synthesis of β-carotene, astaxanthin, and canthaxanthin. Perhaps the same could have occurred in *Trentepohlia aurea*, whereas nitrogen limiting conditions and increasing carotenoid synthesis led to the darkening of the algae. According to the data collected in this study, further studies should focus on more detailed analyses of the carotenoid pool in relation to various nitrogen sources provided.

Estimation of total carotenoids volume. To our knowledge, our study is the first characterizing carotenoids volumes in *Trentepohlia* with CLSM combined with ImageJ. By applying this method, we were able to provide new insights into the carotenoids disposition in the cellular lumen. Our observation shows that cultures grown in medium nitrogen depleted and fully enriched show a similar total carotenoids synthesis, with cultures treated with BG11_0 being slightly higher, the results are statistically significant (Fig 20). Stress inducing factors such as N-limitation, high light intensity and high salinity have been proved to induced synthesis of secondary carotenoids (Bhosale. 2004, Borowitzka et al. 1991). For example *H.pluvialis* in condition of P and N starvation was able to increase its carotenoids production of 40 times (Boussiba et al. 1999) Beside environmental physical factors, nutrients supply is an important factor for carotenoid production. Furthermore nitrogen deficiency conditions have been observed to have a bigger impact than optimum nitrogen conditions regarding carotenoids production (Minhas et al. 2016). This is because cultures growing with media rich in nitrogen

require carbon to assimilate nitrogen. Instead, low nitrogen leads to a greater competition for carbon which can be used for the production of carotenoids and proteins (Borowitzka et al. 1991).

Since F_V/F_M is an ideal, non-invasive tool to assess environmental stressors, and carotenoids production is enhanced by environmental stressors, the relationship between Φmax PSII and carotenoids was analysed (Fig 22). Cultures treated with BG11, BG11_0 and R.w seem all to suggest a negative relationship between F_V/F_M and carotenoids volume, suggesting that at an increase of the Φmax PSII correspond a decrease of the carotenoids volume.

CLSM enabled a very detailed visualization of the cell structures and carotenoids disposition. We were able to clearly show the location of the chloroplast, which is twined into the carotenoids. Moreover, carotenoid droplets effectively occupy most of the cellular lumen. Effect of the treatments on the carotenoids vesicles size were observed (Fig 23). A few recent studies focused on *Trentepohlia* cells morphology and phylogeny (Handa et al. 2024) showing the presence of a zoosporangia ostiole (Zhu et al. 2017), cytokinesis (Chapman et al. 2001) thallus shape and position and cellular development (Zhu et al. 2015) . However no recent studies analyse the exact locations of the carotenoids vesicles in the cellular lumen. Further studies should focus more on carotenoids vescicle morphological characteristics and location within the cellular space. No correlation was found between treatments and carotenoids size and vesicles (Fig 23), it is however noticeable how carotenoids size of the vesicles changes, since a certain tendency can be seen. In the present study we propose how nitrogen supply can impact negatively the photosynthetic capacity of *T.aurea* and therefore its growth condition. Moreover, we examined how nitrogen depleted treatments can lead to an increase of the carotenoids content. Most importantly hereby we first propose a different method to analyse carotenoids contents within algae cells by utilizing confocal microscope and pictures elaboration via ImageJ.

Acknowledgements

I want to thank my supervisor for all the support given during the study. I would like to thank the stuff at the CIUS department, faculty of life science in Vienna for providing us with the equipment and the support needed to perform the CLSM observations. Finally I thank the stuff at the research station WasserCluster Lunz, to let us use some of the stations to perform the environmental measurements.

References

Abe K, Mihara H, Hirano M (1998). Characteristics of growth and carotenoid accumulation of the aerial microalga *Trentepohlia aurea* in liquid culture. *Journal of Marine Biotechnology* 6: 53–58.

Abe, K., Hattori, H., & Hirano, M. (2007). Accumulation and antioxidant activity of secondary carotenoids in the aerial microalga *Coelastrella striolata* var. multistriata. *Food chemistry*, 100(2), 656-661.

Abe, K., Nishimura, N., & Hirano, M. (1999). Simultaneous production of β-carotene, vitamin E and vitamin C by the aerial microalga *Trentepohlia aurea*. *Journal of applied phycology*, 11(4), 331-336.

Abe, K., Imamaki, A., & Hirano, M. (2002). Removal of nitrate, nitrite, ammonium and phosphate ions from water by the aerial microalga *Trentepohlia aurea*. *Journal of Applied phycology*, 14, 129-134

Abe, K., Matsumura, I., Imamaki, A., & Hirano, M. (2003). Removal of inorganic nitrogen sources from water by the algal biofilm of the aerial microalga *Trentepohlia aurea*. *World Journal of Microbiology and Biotechnology*, 19, 325-328.

Almeida, J. S., Julio, S. M., Reis, M. A. M., & Carrondo, M. J. T. (1995). Nitrite inhibition of denitrification by *Pseudomonas fluorescens*. *Biotechnology and bioengineering*, *46*(3), 194-201.

Asada, Kozi. (1999). "The water-water cycle in chloroplasts: scavenging of active oxygens and dissipation of excess photons." *Annual review of plant biology* 50, no. 1: 601-639.

Asada, Kozi. (2000). The water–water cycle as alternative photon and electron sinks. *Philosophical Transactions of the Royal Society of London*. *Series B*: *Biological Sciences*, 355(1402), 1419-1431.

Bankhead, Peat (2022 – 2024). ImageJ: Multidimensional processing.

Bailey, S., Melis, A., Mackey, K. R., Cardol, P., Finazzi, G., van Dijken, G., ... & Grossman, A. (2008). Alternative photosynthetic electron flow to oxygen in marine Synechococcus. *Biochimica et Biophysica Acta (BBA)-Bioenergetics*, *1777*(3), 269-276.

Barker, D. H., Adams III, W. W., Demmig-Adams, B., Logan, B. A., Verhoeven, A. S., & Smith, S. D. (2002). Nocturnally retained zeaxanthin does not remain engaged in a state primed for energy dissipation during the summer in two Yucca species growing in the Mojave Desert. *Plant, Cell & Environment*, *25*(1), 95-103.

Badger, M. R., von Caemmerer, S., Ruuska, S., & Nakano, H. (2000). Electron flow to oxygen in higher plants and algae: rates and control of direct photoreduction (Mehler reaction) and rubisco oxygenase. *Philosophical Transactions of the Royal Society of London. Series B: Biological Sciences*, *355*(1402), 1433-1446.

Belotti, G., Bravi, M., de Caprariis, B., de Filippis, P., & Scarsella, M. (2013). Effect of nitrogen and phosphorus starvations on *Chlorella vulgaris* lipids productivity and quality under different trophic regimens for biodiesel production. *American Journal of Plant Sciences*, 2013.

Bhosale, P. (2004). Environmental and cultural stimulants in the production of carotenoids from microorganisms. *Applied microbiology and biotechnology*, *63*, 351-361.

Boussiba, S., Bing, W., Yuan, J. P., Zarka, A., & Chen, F. (1999). Changes in pigments profile in the green alga *Haeamtococcus pluvialis* exposed to environmental stresses. *Biotechnology Letters*, *21*, 601-604.

Borowitzka, M. A., Huisman, J. M., & Osborn, A. (1991). Culture of the astaxanthin-producing green alga *Haematococcus pluvialis* 1. Effects of nutrients on growth and cell type. *Journal of Applied Phycology*, *3*, 295-304.

Bradbury, M., & Baker, N. R. (1981). Analysis of the slow phases of the in vivo chlorophyll fluorescence induction curve. Changes in the redox state of photosystem II electron acceptors and fluorescence emission from photosystems I and II. *Biochimica et Biophysica Acta (BBA)-Bioenergetics*, 635(3), 542-551.

Butler, W. L. (1978). Energy distribution in the photochemical apparatus of photosynthesis. *Annual Review of Plant Physiology*, 29(1), 345-378.

Brestic, M., & Zivcak, M. (2013). PSII fluorescence techniques for measurement of drought and high temperature stress signal in crop plants: protocols and applications. *In Molecular stress physiology of plants* (pp. 87-131). India: Springer India.

Centonze, V., & Pawley, J. (1995). Tutorial on practical confocal microscopy and use of the confocal test specimen. *Handbook of biological confocal microscopy*, 549-569.

Chapman, R. L., & Good, B. H. (1978). Ultrastructure of plasmodesmata and cross walls in *Cephaleuros*, *Phycopeltis* and *Trentepohlia* (Chroolepidaceae; Chlorophyta). *British phycological journal*, 13(3), 241-246.

Chapman, R. L. (1984). An assessment of the current state of our knowledge of the Trentepohliaceae. *Systematics of the green algae*

Chapman, R. L., Borkhsenious, O., Brown, R. C., Henk, M. C., & Waters, D. A. (2001). Phragmoplast-mediated cytokinesis in *Trentepohlia*: results of TEM and immunofluorescence cytochemistry. *International journal of systematic and evolutionary microbiology*, 51(3), 759-765

Chen, W., Zhang, Q., & Dai, S. (2009). Effects of nitrate on intracellular nitrite and growth of *Microcystis aeruginosa*. *Journal of Applied Phycology*, *21*(6), 701-706.

Cheng, L., Fuchigami, L. H., & Breen, P. J. (2001). The relationship between photosystem II efficiency and quantum yield for CO2 assimilation is not affected by nitrogen content in apple leaves. *Journal of Experimental Botany*, *52*(362), 1865-1872.

Claxton, N. S., Fellers, T. J., & Davidson, M. W. (2006). Laser scanning confocal microscopy. *Encyclopedia of Medical Devices and Instrumentation*, 21(1), 1-37.

Converti, A., Casazza, A. A., Ortiz, E. Y., Perego, P., & Del Borghi, M. (2009). Effect of temperature and nitrogen concentration on the growth and lipid content of *Nannochloropsis oculata* and *Chlorella vulgaris* for biodiesel production. *Chemical Engineering and Processing: Process Intensification*, 48(6), 1146-1151.

Czeczuga, B., & Maximov, O. M. (1996). Carotenoids in the cells of the alga *Trentepohlia gobii* Meyer. *Acta societatis botanicorum poloniae*, 65(3-4), 273-276.

Demmig, B., & Björkman, O. (1987). Comparison of the effect of excessive light on chlorophyll fluorescence (77K) and photon yield of O 2 evolution in leaves of higher plants. *Planta*, 171, 171-184.

De Wildeman, E. (1888). Sur quelques formes du genre *Trentepohlia*. Bull. Soc. R. Bot. Belg. 27:178–82.

Dietz, K. J., Schreiber, U., & Heber, U. (1985). The relationship between the redox state of QA and photosynthesis in leaves at various carbon-dioxide, oxygen and light regimes. *Planta*, 166, 219-226.

Downing, J.A., 2014. Productivity of freshwater ecosystems and climate change. In: Global Environmental Change: *Springer Netherlands*, pp. 221–229.

Eberhard, S., Finazzi, G., & Wollman, F. A. (2008). The dynamics of photosynthesis. *Annual review of genetics*, 42, 463-515.

Ehleringer, J., & Björkman, O. (1977). Quantum yields for CO2 uptake in C3 and C4 plants: dependence on temperature, CO2, and O2 concentration. *Plant Physiology*, 59(1), 86-90.

Eichelmann, Hillar, Vello Oja, R. B. Peterson, and A. Laisk. (2011). "The rate of nitrite reduction in leaves as indicated by O2 and CO2 exchange during photosynthesis." *Journal of Experimental Botany* 62, no. 6 (2011): 2205-2215.

Fernandez, E., & Galvan, A. (2007). Inorganic nitrogen assimilation in Chlamydomonas. *Journal of experimental botany*, 58(9), 2279-2287.

Fritsch, F. E. (1907). The subaerial and freshwater algal flora of the tropics. A phytogeographical and ecological study. *Annals of botany*, 21(82), 235-275.

Fritsch, F. E. (1935). The structure and reproduction of the algae volume I, Introduction, Clorophyceae, Xanthophyceas, chrysophyceae, Bacillariophyceae, Cryptophyceae, Dinophyceae, Chloromanadineae, euglenineae, Colourless flagellata: Volume II, Foreword, Phaephyceae, Rhodophyceae, Myxophycea. *Cambridge University Press.*

Geider, R. J., Macintyre, H. L., Graziano, L. M., & McKAY, R. M. L. (1998). Responses of the photosynthetic apparatus of *Dunaliella tertiolecta* (Chlorophyceae) to nitrogen and phosphorus limitation. *European Journal of phycology*, 33(4), 315-332.

Genty, B., Briantais, J. M., & Baker, N. R. (1989). The relationship between the quantum yield of photosynthetic electron transport and quenching of chlorophyll fluorescence. *Biochimica et Biophysica Acta (BBA)-General Subjects*, 990(1), 87-92.

Gigova, L. G., & Ivanova, N. J. (2015). Microalgae respond differently to nitrogen availability during culturing. *Journal of Biosciences, 40*, 365-374.

Goldman, R. D., & Spector, D. L. (2005). Live cell imaging: a laboratory manual. *Cold Spring Harbor Laboratory Press.*

Gonzalez-Camejo, J., Montero, P., Aparicio, S., Ruano, M. V., Borrás, L., Seco, A., & Barat, R. (2020). Nitrite inhibition of microalgae induced by the competition between microalgae and nitrifying bacteria. *Water Research*, 172, 115499.

Graham, L. E., & McBride, G. E. (1975). the ultrastructure of multilayered structures associated with flagellar bases in motile cells of *trentepohlia aurea* 1. *Journal of phycology*, 11(1), 86-96.

Graham, L. E., & McBride, G. E. (1978). mitosis and cytokinesis in sessile sporangium of *trentepohlia aurea* (chlorophyceae) 1. *Journal of Phycology*, 14(2), 132-137

Guiry, M. D., and Guiry, G. M. 2015. *AlgaeBase*. Worldwide electronic publication, National University of Ireland, Galway. Retrieved on March 25, 2015 from: http://www.algaebase.org/

Gupta, S., & Agrawal, S. C. (2004). Vegetative survival and reproduction under submerged and air-exposed conditions and vegetative survival as affected by salts, pesticides, and metals in aerial green alga *Trentepohlia aurea*. *Folia microbiologica*, 49, 37-40.

Handa, S., Nakahara-Tsubota, M., Shoda, I., Mizobuchi, A., Nakano, T., & Tsubota, H. (2024). *Trentepohlia brevicellulis* comb. et stat. nov.(Trentepohliaceae, Ulvophyceae) found in Japan. Phycological Research, 72(1), 12-26.

Hariot, P. (1889). Notes sur le genre *Trentepohlia* Martius. J. Bot., Paris, 3, 345-50

Havaux, M., & Niyogi, K. K. (1999). The violaxanthin cycle protects plants from photooxidative damage by more than one mechanism. *Proceedings of the National Academy of Sciences*, 96(15), 8762-8767.

Havaux, M., Dall'Osto, L., & Bassi, R. (2007). Zeaxanthin has enhanced antioxidant capacity with respect to all other xanthophylls in Arabidopsis leaves and functions independent of binding to PSII antennae. *Plant physiology*, *145*(4), 1506-1520.

Hazrati, S., Tahmasebi-Sarvestani, Z., Modarres-Sanavy, S. A. M., Mokhtassi-Bidgoli, A., & Nicola, S. (2016). Effects of water stress and light intensity on chlorophyll fluorescence parameters and pigments of Aloe vera L. *Plant Physiology and Biochemistry*, 106, 141-148.

Hemschemeier, A., & Happe, T. (2011). Alternative photosynthetic electron transport pathways during anaerobiosis in the green alga Chlamydomonas reinhardtii. *Biochimica et Biophysica Acta (BBA)-Bioenergetics*, 1807(8), 919-926.

Ho, K. K., Tan, K. H., & Wee, Y. C. (1983). Growth conditions of *Trentepohlia odorata* (Chlorophyta, Ulotrichales). *Phycologia*, 22(3), 303-308.

Hoek, C., Mann, D., Jahns, H. M., & Jahns, M. (1995). Algae: an introduction to phycology. *Cambridge university press.*

Holzinger, Andreas, Niklas Plag, Ulf Karsten, and Karin Glaser. "Terrestrial *Trentepohlia sp*.(Ulvophyceae) from alpine and coastal collection sites show strong desiccation tolerance and broad light and temperature adaptation." *Protoplasma* (2023): 1-15.

Howland, L. J. (1929). The moisture relations of terrestrial algae. IV. Periodic observations of *Trentepohlia aurea*, Martius. *Annals of Botany*, 43(169), 173-202.

Hwang, D. F., & Lu, Y. H. (2000). Influence of environmental and nutritional factors on growth, toxicity, and toxin profile of dinoflagellate *Alexandrium minutum*. *Toxicon*, *38*(11), 1491-1503.

Kharkongor, D., & Ramanujam, P. (2014). Diversity and species composition of subaerial algal communities in forested areas of Meghalaya, India. *International Journal of Biodiversity*, *2014*(1), 456202.

Kharkongor, D., & Ramanujam, P. (2015). Spatial and temporal variation of carotenoids in four species of *Trentepohlia* (Trentepohliales, Chlorophyta). *Journal of Botany*, 2015.

Kızılkaya, İ. T., & Unal, D. (2019). Effects of Nitrate toxicity on free Proline accumulation, chlorophyll degradation and photosynthetic efficiency in *Chlorella vulgaris* Beyerinck [Beijerinck]. *International Journal of Secondary Metabolite*, 6(1), 10-19.

Klyachko-Gurvich, G. L., Pronina, N. A., Tsoglin, L. N., Semenenko, V. E., & Ladygin, V. G. (2000). Uncoupled functioning of separate photosystems: 1. Characteristics of fatty acid desaturation and its role. *Russian Journal of Plant Physiology*, *47*(5), 603-612.

Lang, Y., Wang, M., Xia, J., & Zhao, Q. (2018). Effects of soil drought stress on photosynthetic gas exchange traits and chlorophyll fluorescence in Forsythia suspensa. *Journal of Forestry Research*, 29, 45-53.

Ladygin, V. G. (2014). Ways of biosynthesis, localization, metabolism and functions of carotenoids in chloroplasts of different types of algae. *Issues Mod. Algol*, *2*.

López-Bautista JM, Waters DA, Chapman RL (2002) The Trentepohliales revisited. Constancea 83. Available: http://ucjepsberkeleyedu/constancea/83/ lopezetal/trentepohliales html

Lachmann, S. C., Mettler-Altmann, T., Wacker, A., & Spijkerman, E. (2019). Nitrate or ammonium: Influences of nitrogen source on the physiology of a green alga. *Ecology and evolution*, *9*(3), 1070-1082.

López-Bautista, J. M. (2008). Subaerial algae in tropical rainforests. University of Alabama.

Loranger, C., & Carpentier, R. (1994). A fast bioassay for phytotoxicity measurements using immobilized photosynthetic membranes. *Biotechnology and bioengineering*, *44*(2), 178-183.

Manton, I. R. E. N. E. (1966). Some phyletic implications of flagellar structure in plants. *In Advances in botanical research* (Vol. 2, pp. 1-34). Academic Press.

Martius K. Ph (1817). Flora Cryptogamica erlangensins sistens vegelarla e classe ultima Linn. in agro Eragensi. J. L. Schrag, Nurembra. 501 pp.

Masters, B. R. (1996). Selected papers on confocal microscopy. *SPIE milestone series*, 131.

Minhas, A. K., Hodgson, P., Barrow, C. J., & Adholeya, A. (2016). A review on the assessment of stress conditions for simultaneous production of microalgal lipids and carotenoids. *Frontiers in microbiology*, 7, 183978.

Miyake, C. (2010). Alternative electron flows (water–water cycle and cyclic electron flow around PSI) in photosynthesis: molecular mechanisms and physiological functions. *Plant and Cell Physiology*, 51(12), 1951-1963.

Murchie, E. H., & Lawson, T. (2013). Chlorophyll fluorescence analysis: a guide to good practice and understanding some new applications. *Journal of experimental botany*, 64(13), 3983-3998.

Mushtaq, N., Singh, D. V., Bhat, R. A., Dervash, M. A., & Hameed, O. B. (2020). Freshwater contamination: sources and hazards to aquatic biota. *Fresh water pollution dynamics and remediation*, 27-50.

Mukherjee, R., Borah, S. P., & Goswami, B. C. (2010). Biochemical characterization of carotenoids in two species of *Trentepohlia* (Trentepohliales, Chlorophyta). *Journal of applied phycology*, 22, 569-571.

Nelson, N., & Yocum, C. F. (2006). Structure and function of photosystems I and II. *Annu. Rev. Plant Biol.*, *57*(1), 521-565.

Oltmanns, F. (1923). Morphologie und biologie der algen (Vol. 3). G. Fischer.

Ong, B. L., Lim, M., & Wee, Y. C. (1992). Effects of desiccation and illumination on photosynthesis and pigmentation of an edaphic population of *Trentepohlia odorata* (Chlorophyta) 1. *Journal of phycology*, 28(6), 768-772.

O'Neill, P. M., Shanahan, J. F., & Schepers, J. S. (2006). Use of chlorophyll fluorescence assessments to differentiate corn hybrid response to variable water conditions. *Crop Science*, 46(2), 681-687.

Ort, D. R., & Baker, N. R. (2002). A photoprotective role for O2 as an alternative electron sink in photosynthesis?. *Current opinion in plant biology*, *5*(3), 193-198.

Otsu, N. (1975). A threshold selection method from gray-level histograms. *Automatica*, *11*(285-296), 23-27.

Owens, T.G., Shreve, A.P., and Albrecht, A.C. (1992). Dynamics and mechanism of singlet energy transfer between carotenoids and chlorophyll: light harvesting and non photochemical fluorescence quenching, in Research in Photosynthesis, Murata, N., Ed., Dordrecht: Kluwer vol. 1, pp. 171–178.

Parkhill, J. P., Maillet, G., & Cullen, J. J. (2001). Fluorescence-based maximal quantum yield for PSII as a diagnostic of nutrient stress. *Journal of Phycology*, 37(4), 517-529.

Printz, H. (1921). Subaerial algae from south Africa. K. Norske Vidensk. Selsk. Skr. 1:3–41

Printz, H. (1939). Vorarbeiten zu einer Monographie der Trentepohliaceen. na.

Printz, H. (1964). Die chaetophoralen der binnengewässer: eine systematische übersicht. *Hydrobiologia*, 24(1-2), 1-376.

Quick, W. P., & Horton, P. (1984). Studies on the induction of chlorophyll fluorescence in barley protoplasts. II. Resolution of fluorescence quenching by redox state and the transthylakoid pH gradient. *Proceedings of the Royal society of London. Series B. Biological sciences*, 220(1220), 371-382.

R Core Team (2022). R: A language and environment for statistical computing. R Foundation for Statistical Computing, Vienna, Austria.URL https://www.R-project.org/.

Rasband,W.S.(1997-2018). ImageJ, U. S. National Institutes of Health, Bethesda, Maryland, USA, https://imagej.nih.gov/ij/.

Rindi, F. (2007). Diversity, distribution and ecology of green algae and cyanobacteria in urban habitats. *In Algae and cyanobacteria in extreme environments* (pp. 619-638). Dordrecht: Springer Netherlands.

Rindi, F., Lam, D. W., & López-Bautista, J. M. (2009). Phylogenetic relationships and species circumscription in *Trentepohlia* and *Printzina* (Trentepohliales, Chlorophyta). *Molecular phylogenetics and evolution*, 52(2), 329-339

Rindi, F., & Guiry, M. D. (2002). Diversity, Life History, and Ecology of *trentepohlia* and *printzina* (Trentepohliales, Chlorophyta) in Urban Habitats in Western Ireland 1. *Journal of phycology*, 38(1), 39-54.

Rippka, R. (1992). Pasteur culture collection of cyanobacterial strains in axenic culture. *Catalogue and taxonomic handbook, catalogue of strains* 1992/1993, 1, 1-103.

Roberts, K. R. (1984). The flagellar apparatus in *Batophora* and *Trentepohlia* and its phylogenetic significance. *Systematics of the green algae*.

Ruan, Z., & Giordano, M. (2017). The use of NH4+ rather than NO3− affects cell stoichiometry, C allocation, photosynthesis and growth in the cyanobacterium *Synechococcus sp*. UTEX LB 2380, only when energy is limiting. *Plant, cell & environment*, 40(2), 227-236.

Saraphol, S., Vajrodaya, S., Kraichak, E., Sirikhachornkit, A., & Sanevas, N. (2020). Environmental Factors Affecting the Diversity and Photosynthetic Pigments of *Trentepohlia* Species in Northern Thailand's Chiang Dao Wildlife Sanctuary. *Acta Societatis Botanicorum Poloniae*, *89*(1).

Schreiber, U., Schliwa, U., & Bilger, W. (1986). Continuous recording of photochemical and non-photochemical chlorophyll fluorescence quenching with a new type of modulation fluorometer. *Photosynthesis research*, 10, 51-62.

Schreiber, U., & Bilger, W. (1993). Progress in chlorophyll fluorescence research: major developments during the past years in retrospect. *Progress in Botany/Fortschritte der Botanik: Structural Botany Physiology Genetics Taxonomy Geobotany/Struktur Physiologie Genetik Systematik Geobotanik*, 151-173.

Schreiber, U., Hormann, H., Neubauer, C., & Klughammer, C. J. F. P. B. (1995). Assessment of photosystem II photochemical quantum yield by chlorophyll fluorescence quenching analysis. *Functional Plant Biology*, *22*(2), 209-220.

Schulze ED, Caldwell MM (1994). Ecophysiology of photosynthesis. (Ecological Studies, vol 100) Springer, Berlin Heidelberg New York

Shi, Y., Hu, H., & Cong, W. (2005). Positive effects of continuous low nitrate levels on growth and photosynthesis of *Alexandrium tamarense* (Gonyaulacales, Dinophyceae). *Phycological Research*, 53(1), 43-48.

Spiller, H., & Böger, P. (1977). Photosynthetic nitrite reduction by dithioerythritol and the effect of nitrite on electron transport in isolated chloroplasts. *Photochemistry and Photobiology*, *26*(4), 397-402.

Streb P, Josse E-M, Galloue¨t E, Baptist F, Kuntz M, Cornic G. (2005).Evidence for alternative electron sinks to photosynthetic carbon assimilation in the high mountain plant species *Ranunculus glacialis*. *Plant, Cell Environ* 28:1123–1135

Tan, C. K., Lee, Y. K., & Ho, K. K. (1993). Effect of light intensity and ammonium-N on carotenogenesis of *Trentepohlia odorata* and *Dunaliella bardawil*. *Journal of applied phycology*, 5(5), 547-549.

Thompson, R. H., & Wujek, D. E. (1997). Trentepohliales: Cephaleuros, Phycopeltis, and Stomatochroon: morphology, taxonomy, and ecology. Science publishers.

Turpin, D. H., Elrifi, I. R., Birch, D. G., Weger, H. G., & Holmes, J. J. (1988). Interactions between photosynthesis, respiration, and nitrogen assimilation in microalgae. *Canadian Journal of Botany*, *66*(10), 2083-2097.

Tylova-Munzarova, E., Lorenzen, B., Brix, H., & Votrubova, O. (2005). The effects of NH4+ and NO3− on growth, resource allocation and nitrogen uptake kinetics of *Phragmites australis* and *Glyceria maxima*. *Aquatic Botany*, 81(4), 326-342.

Verhoeven, J. W. (1996). Glossary of terms used in photochemistry (IUPAC Recommendations 1996). *Pure and Applied Chemistry*, 68(12), 2223-2286.

Villani Thomas. Blog Post: Loading and Measurement of Volumes in 3D Confocal Image Stacks with ImageJ. https://visikol.com/blog/2018/11/29/blog-post-loading-and-measurement-of-volumes-in-3d-confocal-image-stacks-with-imagej/

VSIKOL.https://visikol.com/blog/2018/11/29/blog-post-loading-and-measurement-of-volumes-in-3d-confocal-image-stacks-with-imagej/

Voytsekhovich, A. A., & Kashevarov, G. P. (2010). Pigment content of photosynthetic apparatus of green algae (Chlorophyta)-the photobionts of lichens. *International journal on algae*, 12(3).

Wang, J., Zhou, W., Chen, H., Zhan, J., He, C., & Wang, Q. (2019). Ammonium nitrogen tolerant Chlorella strain screening and its damaging effects on photosynthesis. Frontiers in Microbiology, 9, 3250.

Weis, E., & Berry, J. A. (1987). Quantum efficiency of photosystem II in relation to 'energy'-dependent quenching of chlorophyll fluorescence. *Biochimica et Biophysica Acta (BBA)-Bioenergetics*, 894(2), 198-208.

Wille, J. N. F. (1878). Om svaermecellerne og deres copulation hos *Trentepohlia* Mart.

Yang, S., Wang, J., Cong, W., Cai, Z., & Ouyang, F. (2004). Utilization of nitrite as a nitrogen source by *Botryococcus braunii*. *Biotechnology letters*, *26*, 239-243.

Zhu, H., Zhao, Z., Xia, S., Hu, Z., & Liu, G. (2015). Morphological examination and phylogenetic analyses of *Phycopeltis spp*.(Trentepohliales, Ulvophyceae) from tropical China. *Plos one*, *10*(2), e0114936.

Zhu, H., Hu, Z., & Liu, G. (2017). Morphology and molecular phylogeny of Trentepohliales (Chlorophyta) from China. *European Journal of Phycology*, *52*(3), 330-341

German abstract

Trentepohlia aurea, aufgrund ihres extrem hohen Gehalts an Carotinoiden, hat sich als interessanter Organismus für die kommerzielle Nutzung erwiesen. Merkmale wie der aeroterrestrische Lebensraum, die Toleranz gegenüber Austrocknung und die Synthese wertvoller Verbindungen wie β-Carotin, Vitamin C und Vitamin E machen sie zu einem vielversprechenden Forschungstaxon. Wir haben die maximale Quantenausbeute des Photosystems II und das Volumen der zellulären Carotinoid-Vesikel von *T. aurea* unter verschiedenen Behandlungen untersucht (BG11, BG11 in 1/10 Konzentration und BG11 stickstoffdepletiert). Signifikante Unterschiede zwischen Kulturen, die unter stickstofflimitierten Bedingungen behandelt wurden, und anderen Behandlungen wurden festgestellt, wobei *T. aurea* eine deutlich höhere maximale Quantenausbeute des PSII und eine Zunahme der Gesamtcarotinoide zeigte. Darüber hinaus wurden verschiedene Substrate getestet (Agar und Marmolade), wobei Marmolade sich als bestes Substrat für das Wachstum der Alge erwies. Beobachtungen des Chloroplasten und der Carotinoid-Lokalisierungen innerhalb der Zellen mittels konfokaler Laser-Scanning-Mikroskopie ermöglichten uns die Berechnung der Volumina der Carotinoid-Vesikel. Zudem stellen wir hier einen Rahmen zur Messung des Carotinoid-Vesikel-Volumens vor, indem Stack images mit einem konfokalen Mikroskop aufgenommen und mithilfe von ImageJ ausgewertet werden.